LIT-001, the First Nonpeptide Oxytocin Receptor Agonist that Improves Social Interaction in a Mouse Model of Autism

Marie-Céline Frantz, Lucie P. Pellissier, Elsa Pflimlin, Stéphanie Loison, Jorge Gandía, Claire Marsol, Thierry Durroux, Bernard Mouillac, Jérôme Becker, Julie Le Merrer, et al.

Journal of Medicinal Chemistry

Article

Cite This: J. Med. Chem. 2018, 61, 8670−8692

pubs.acs.org/jmc

LIT-001, the First Nonpeptide Oxytocin Receptor Agonist that Improves Social Interaction in a Mouse Model of Autism

Marie-Céline Frantz,[†,#] Lucie P. Pellissier,[‡,#] Elsa Pflimlin,[†,#] Stéphanie Loison,[†,#] Jorge Gandía,[‡] Claire Marsol,[†,∥,⊥] Thierry Durroux,[§] Bernard Mouillac,[§] Jérôme A. J. Becker,[‡] Julie Le Merrer,[‡] Christel Valencia,[∥,⊥] Pascal Villa,[∥,⊥] Dominique Bonnet,[†,∥] and Marcel Hibert*[,†,∥]

[†]Laboratoire d'Innovation Thérapeutique, Faculté de Pharmacie, UMR7200 CNRS/Université de Strasbourg, 74 Route du Rhin, F-67412 Illkirch, France

[‡]Physiologie de la Reproduction et des Comportements, INRA UMR-0085, CNRS UMR-7247, IFCE, Inserm, Université François Rabelais de Tours, F-37380 Nouzilly, France

[§]Institut de Génomique Fonctionnelle, CNRS UMR5203, INSERM U661, Université de Montpellier (IFR3), 141 Rue de la Cardonille, F-34094 Montpellier Cedex 5, France

[∥]LabEx MEDALIS, Université de Strasbourg, F-67000 Strasbourg, France

[⊥]PCBIS Plateforme de Chimie Biologique Intégrative de Strasbourg, UMS3286, CNRS/Université de Strasbourg, F-67000 Strasbourg, France

Supporting Information

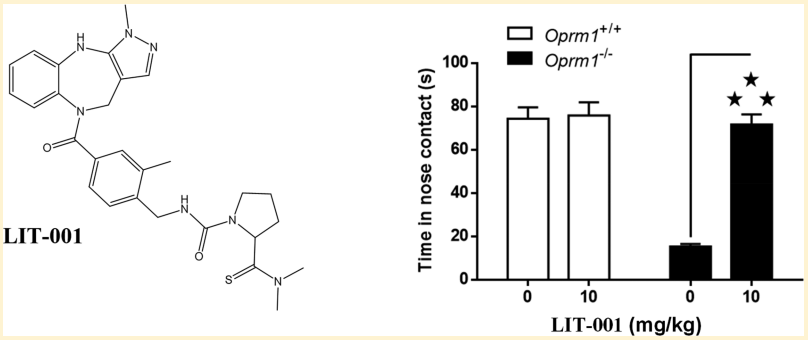

ABSTRACT: Oxytocin (OT) and its receptor (OT-R) are implicated in the etiology of autism spectrum disorders (ASD), and OT-R is a potential target for therapeutic intervention. Very few nonpeptide oxytocin agonists have currently been reported. Their molecular and in vivo pharmacology remain to be clarified, and none of them has been shown to be efficient in improving social interaction in animal models relevant to ASD. In an attempt to rationalize the design of centrally active nonpeptide full agonists, we studied in a systematic way the structural determinants of the affinity and efficacy of representative ligands of the V_{1a} and V_2 vasopressin receptor subtypes (V_{1a}-R and V_2-R) and of the oxytocin receptor. Our results confirm the subtlety of the structure−affinity and structure−efficacy relationships around vasopressin/oxytocin receptor ligands and lead however to the first nonpeptide OT receptor agonist active in a mouse model of ASD after peripheral ip administration.

INTRODUCTION

Autism spectrum disorders (ASD) are neurodevelopment diseases characterized by impaired social interaction and communication together with repetitive behaviors and restricted social interest (American Psychiatric Association, 2013). These core symptoms must be present in the early developmental period (by 3 years of age) for the diagnosis of ASD to be made. The prevalence of ASD is currently estimated at 1 case for 88 births, however, with a very large diversity of the associated mental disorders.[1,2] The etiology of ASD is complex. Hundreds of genetic mutations have been associated with the disease, explaining a number of ASD cases.[3] The identification of vulnerability genes, most of them coding for proteins involved in synaptic function, as well as environmental risk factors during pregnancy and development, has provided important insights into the understanding of the anatomical and molecular underpinnings of ASD, notably by giving access to valuable animal models.[4−7] However, most of the etiopathological mechanisms leading to ASD remain to be identified. The social impact of ASD is huge. U.S. annual direct medical, direct nonmedical, and productivity costs combined will be $268 billion for 2015 and $461 billion for 2025.[8]

Up to now, no drug has been approved to treat core symptoms of ASD. Antipsychotics (aripiprazol, risperidone) or antidepressants (fluoxetine, citalopram) are often administered to

Received: May 2, 2018
Published: September 10, 2018

DOI: 10.1021/acs.jmedchem.8b00697
J. Med. Chem. 2018, 61, 8670−8692

treat some of the severe associated symptoms such as irritability and compulsive, repetitive behaviors, respectively, with associated side effects (drowsiness, weight gain, etc.). Novartis has developed up to phase II clinical trial an mGluR5 inhibitor, mavoglurant, showing a very marginal improvement in Fragile X patients diagnosed with ASD. Unfortunately, trial results did not meet the primary end point of showing significant improvement in abnormal behaviors compared to placebo and the development has been stopped.[9] Similarly, arbaclofen, the R enantiomer of baclofen, showed little effect on irritability subscale and development was stopped after phase IIb studies.[10] Balovaptan is a promising drug candidate developed by Hoffmann-La Roche and entering a phase III clinical study in ASD adults (https://clinicaltrials.gov/ct2/show/NCT03504917) with a FDA Breakthrough Therapy designation. This compound is claimed to be a specific V_{1a} receptor antagonist. Unfortunately, no preclinical pharmacological data have been published yet to support its mechanism of action. The effect of a diuretic, bumetanide, blocking GABA-gated chloride channels, has recently been reported by Ben Ari et al. and looks promising.[11,12] Interestingly, there is a clear relationship between this signaling pathway and oxytocin.[12] Furthermore, many studies in patients demonstrate that OT may significantly improve social abilities related to autism spectrum.[13−35] These studies differ significantly in terms of age and gender of participants, administration route (intravenous or intranasal), doses of OT, single or multiple long-term administration, and outcomes (repetitive behavior, comprehension of affective speech, social ball tossing game, reading the mind in eyes, etc.), making definitive conclusions difficult to draw. However, OT clearly appears as a promising target to alleviate social impairments in patients with ASD.[36]

Surprisingly, these OT clinical trials are running while very little is known about the precise molecular pharmacology, pharmacokinetics, and pathophysiological functions of OT in animals and in man. Understanding the distribution and functions of this neurotransmitter is crucial for the meaningful interpretation of animal and clinical studies and to rationalize the design of better drug candidates. For instance, no OT-R specific brain penetrating positron emission tomography (PET) probe is currently available.[37,38] Furthermore, the only way to get central activity with OT is intranasal (i.n.) administration because, as with most peptides, OT is not orally absorbed,[39] is rapidly metabolized after iv administration (few minutes),[40] and poorly crosses blood−brain barrier except very modestly via the intranasal route.[41,42] That is far from ideal in terms of formulation because the actual concentrations of OT being administered and reaching the different brain regions are unknown.[42] In addition, the pharmacodynamics of this hormone is poorly documented. Thus, OT has very similar affinities for its OT-R and for the vasopressin receptors V_{1a}-R and V_{1b}-R and it is not fully understood which receptor is indeed associated with the different OT functions.[43−45] Furthermore, these receptors are able to activate different signaling pathways (different G proteins, arrestin), and the relationship between these pathways and the different physiological functions mediated by OT remains to be better understood.[43−45]

Finally, it is very unlikely that OT could ever be marketed to treat ASD because performing full dedicated clinical trials would be very costly while intellectual property cannot be protected.

These different elements indicate that there is a clear need to discover novel centrally active, nonpeptide OT agonists both for fundamental research and for drug development.

Consequently, our aim was to design and develop a novel nonpeptide OT-R agonist active in animal models of autism after peripheral administration. To our knowledge, no compound with such a profile has yet been disclosed. Few peptide or peptide-like OT-R agonists have been described, but their bioavailability is not much improved over OT and their in vivo efficacy in autism models has not been reported.[46,47] Two nonpeptide compounds showing some agonist activity have been discovered by Ferring and Wyeth.[40,48] The Ferring compound is in fact more efficient as a V_{1a}-R antagonist than as OT-R agonist,[49] and its clinical development has been stopped. The Wyeth compound, WAY-267464, has been reported as a high-affinity, potent, and selective (vs V_{1a}, V_{1b}, V_2) agonist of the OT receptor in a given experimental system.[40] It is more and more often used and referenced as a selective full OT-R agonist.[50] However, in a different experimental setup, this compound was found to have an 8-fold higher affinity for the V_{1a} receptor with a poor functional selectivity (2× selective for OT-R agonism over V_{1a}-R antagonism)[51] and partial OT agonism (see below). Our own efforts to discover OT-R agonists by virtual[52] and biological high throughput screening of diverse libraries or by rational design of oxytocin mimics failed. Actually, OT-R ligands were found but none of them showed agonist activity (unpublished results and ref 52). We came back to a more classical approach in looking for a common basic pharmacophore among ligands of vasopressin/oxytocin receptors as a starting template to develop a full OT agonist. In our eyes, this makes sense because there is a high sequence similarity between the three vasopressin receptor subtypes and the oxytocin receptor that all belong to the same branch of the GPCR family.[53] On the other hand, vasopressin and oxytocin bind with moderate to high affinity to these four receptors. Furthermore, Table 1 shows that compounds with similar structures have already been characterized as high affinity ligands of one or several of these four receptor subtypes.[40,48,51,54−61] A simple examination of these representative series of ligands reveals that a benzoyl benzazepine pharmacophore is clearly shared by this set of molecules showing affinity for at least one member of the vasopressin/oxytocin receptor family. Most compounds are antagonists except VNA-932 and WAY-141608 that display V_2 receptor agonism[54,55] and the Ferring and Wyeth OT partial agonists.[48,51] Thus, this arylacyl benzazepine pharmacophore seems appropriate to afford improved OT agonists. In addition, compared to OT, it displays the potential advantages of structural simplicity, low molecular weight, and druglikeness.

We report here the binding and efficacy studies around the pharmacophore of V_{1a}, V_{1b}, V_2, and OT receptor ligands using three series of compounds with (i) variations of the side chain on the 4-position of the simplest benzoylbenzazepine pharmacophoric nucleus (Table 2), (ii) variations on the benzazepine fragment keeping the pyrazole side chain selected previously (Table 3), and (iii) variation of the side chain of the pyrazolobenzodiazepine fragment selected on OT agonism potential (Table 4). This led to the first identification of a new nonpeptide OT-R agonist, active in a mouse model of autism after peripheral intraperitoneal administration.

RESULTS

Chemistry. *Benzazepine Derivatives.* Benzazepine derivatives were prepared by coupling benzazepine **8** with a series of substituted aryl acids synthesized as indicated in Scheme 1. The acid precursors **3a**,**b** were prepared according to the method

DOI: 10.1021/acs.jmedchem.8b00697
J. Med. Chem. 2018, 61, 8670−8692

Table 1. Selection of Literature Vasopressin/Oxytocin Ligands with the Benzoylbenzazepine Pharmacophore

Name[ref]	Structure	Affinity (K_i or IC_{50}, nM) and/or function (agonist: EC_{50}, nM; antagonist: IC_{50}, nM)			
		V_{1a}-R	V_{1b}-R	V_2-R	OT-R
Ferring[48]	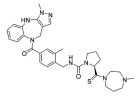	K_i = 330[49]		EC_{50} = 850[48,a] K_i >1000[49]	EC_{50} = 33[48,a] K_i = 147[49]
WAY-267464[40,51]	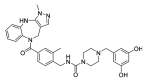	K_i >1000[40] K_i = 113[51]	K_i >1000[40]	K_i >1000[40]	K_i = 58.4[40] EC_{50} = 61.3[40,b] K_i = 978[51]
YM087 or Conivaptan[54]	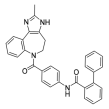	K_i = 0.48[54]	>10000[54]	K_i = 3.04[54]	K_i = 44.4[54]
YM218[55]	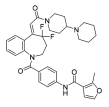	K_i = 0.30[55]	K_i = 25500[55]	K_i = 381[55]	K_i = 71[55]
JNJ17158063[56]	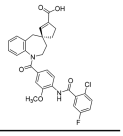	IC_{50} = 5[56]		IC_{50} = 34[56]	
OPC-51803[57]	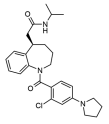	K_i = 819[57]	IC_{50} >100 μM[57]	K_i = 91.9[57] EC_{50} = 189 nM[57]	nd[e]
Yamanouchi[58]	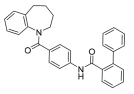	IC_{50} = 2.74	nd[e]	IC_{50} = 0.57	IC_{50} = 109
Otsuka[59]	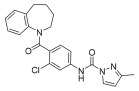	IC_{50} = 19	>1000	IC_{50} = 13 Agonist EC_{50} = 4.0	IC_{50} = 37.0
WAY-VNA-932[60]	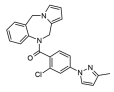	K_i = 465 antagonist IC_{50} = 1660[d]	K_i >1 μM	K_i = 39.9 agonist EC_{50} = 0.7[d]	K_i = 125 antagonist IC_{50} = 55[e]
WAY-141608[61]	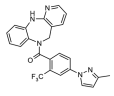	IC_{50} = 5954 antagonist IC_{50} > 30 μM[c]	No activity	IC_{50} = 493 agonist EC_{50} = 1.7[d]	nd antagonist IC_{50} =1259[e]

[a]Gene reporter assay. [b]Changes in intracellular Ca^{2+}. [c]Not determined. [d]cAMP accumulation. [e]Isolated organ (rat artery for V_{1a}-R, rat uterus for OT-R).

described by Kondo et al. (2000).[59] Acid precursors **5a,b** were prepared by Suzuki coupling according to the method of Gong et al. (2000),[62] optimized for microwave conditions.

Benzazepine **8** was prepared from the corresponding oxime **7** as described (Scheme 2).[63] Coupling was achieved by using commercially available acid chlorides (for compounds **9**−**14** and **18**) or starting from prepared acids **3a** and **5a** (for compounds **15**−**17**) using thionyl chloride.[59,64,65] The reduction of the nitro group of **18** was achieved as described by Ogawa et al. (1996).[65] Double methylation of aniline **19** was performed as described by Kondo et al. (2000).[59] Peralkylation of **20** was achieved with methyl iodide and silver perchlorate following a procedure described by Miller et al. (1989),[66] while acetylation of **19** led to **22**. The reference antagonist **23** was obtained by acylation of **19** with 2-biphenylcarboxylic acid as previously described by Matsuhisa et al. (1997).[58] Structures and yields are given in Scheme 2.

Aryl-1-(3-Me)-pyrazolyl Derivatives. A series of compounds resulting from the coupling of substituted 1-(3-Me)-pyrazolyl-benzoic acids **3a,b** with cyclic amines have been prepared. The cyclic amines have been synthesized (Scheme 3) according to existing procedures. Ketone **25** was prepared as described by Proctor et al. (1961).[67] We had already described the synthesis of benzazepinone **26**.[68] *N*-Dimethylbenzazepine **28** was prepared from ketone **25** according to a procedure described by Ogawa et al. (1996).[65] The pyrrolobenzodiazepine **31** was obtained following a procedure described by Artico et al. (1969).[69] The pyrazolobenzodiazepine **37** was prepared according to the method described by Pitt et al. (2004).[48] Azepine is commercially available. The different benzazepines were coupled to the aromatic acids as described before via acyl chloride intermediate (Scheme 4). The V_2 receptor agonist VNA-932 (**42**) was prepared from benzodiazepine **31**.[70] The coupling products **39a** and **39b**, obtained from ketone **26**, were further reduced by sodium borohydride to obtain the alcohols **40a** and **40b**.[64] Structures and yields are given in Scheme 4.

Pyrazolobenzodiazepine Derivatives. A series of amines was prepared according to Scheme 5 and Scheme 6. The first series dealt with proline analogues (Scheme 5). *N*-Boc-proline **45** reacted with *N,N*-dimethylamine to afford the corresponding carboxamide **46** with a 75% yield. The carboxamide **46** was transformed into the corresponding thiocarboxamide **47** with the Lawesson reagent in 52% yield. Finally, Boc protection was removed with TFA/CH_2Cl_2:1/1 to afford quantitatively the building blocks **48** and **49**. A second series of building blocks was derived from glycine (Scheme 6). *N*-Protected glycine was first turned into the *N,N*-dimethyl carboxamide **50** and then into the thiocarboxamide **51** following the same sequence as above for proline derivatives. Deprotection in acidic medium afforded the free amino thiocarboxamide **52** and carboxamide **53** with quantitative yields. The methyl ester of glycine, **54**, was commercially available. The pyrazolobenzodiazepine **37** reacted with 4-cyano-3-methyl benzoic acid chloride to afford compound **55** in a 70% yield (Scheme 7). The cyano group was reduced with sodium borohydride in the presence of cobalt chloride hexahydrate to provide the primary amine **56** with 81% yield. A urea connection was then created with carbonyldiimidazole (CDI) between the amine **56** and the previously synthesized amines **48**, **49**, and **52**−**54**, leading to compounds **57**−**61**. Yields ranged from 41% to 67% (Scheme 7).

Structure−Activity Relationship Studies. The affinities of the different ligands for the human vasopressin receptor subtypes and the oxytocin receptor were determined as described previously (i) on CHO cell membranes by competition experiments against [^{3}H]AVP,[49] and (ii) on HEK cells using a FRET based assay.[71] The functional agonist and competitive antagonist properties of each ligand were determined for the human vasopressin and oxytocin receptor subtypes in different experimental conditions. (i) In CHO cells stably expressing receptors, the accumulation of *myo*-inositol 1-phosphate (V_{1a} and OT receptors) and the accumulation of cAMP (V_2 receptor) were determined using immunoassays

DOI: 10.1021/acs.jmedchem.8b00697
J. Med. Chem. 2018, 61, 8670−8692

Table 2. Affinity and Potency of Benzazepine Derivatives on V_{1a}, V_2, and OT Receptors

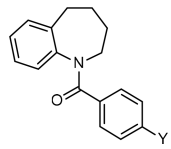

		V_{1a}-R			V_2-R			OT-R		
Cpd	Y	affinity[a]	ago[b]	antago[c]	affinity[a]	ago[b]	antago[c]	affinity[a]	ago[b]	antago[c]
9	Cl	556±143	ns	149±45	507±26	15±7%	39±12%	ns	ns	24.1±0.1%
10	Br	504±137	ns	218±38	713±76	17±6%	25±9%	ns	ns	20±10%
11	I	48±10	ns	15±3	160±57	25±7%	44±6%	396±117	ns	36±2%
12	*n*Pr	63±14	ns	184±36	121±6	92±27 64±3%	ns	104±22	ns	172±81
13	*n*Bu	28±11	ns	421±68	52±9	18±5 74.0±0.3%	ns	37.4±1.6	ns	113±15[g]
14		2.28±0.51	ns	7±4[f]	78±14	17±8%	132±32	10.4±0.9	ns	42±4[g]
15		67±12	ns	51±5	233±8	12±6%	78±22[f]	150±53	ns	227±94
16		573±45	ns	177±27	334±5	23±8%	26±9%	340±35	ns	30.56±0.06 %
17		34±3	ns	48±8	282±11	13±4 99±3%	ns	84±13	ns	112±8
19	NH_2	734±52	ns	37±2%	>1000	ns	ns	ns	ns	15±12%
20		82±5	ns	81±23	468±3	80±15 84±2%	ns	>1000	ns	186±11
21		>1000[d]	ns	15±9%	>1000	ns	ns	ns	ns	19±2%
22		1075[e]	ns	305±63	>1000	ns	ns	>1000	ns	32±8%[f]
23		2.74±0.19	ns	63±8	0.57±0.18	ns	0.096±0.030	109±34	ns	171±29

[a]The inhibition constants (K_i in nM) for human V_{1a}, V_2, and OT receptors were determined on CHO cell membranes by competition binding assays (displacement of radioactive [^{3}H]AVP). Results are expressed as mean ± SEM of at least three separate experiments performed in triplicate. When K_i >1000 or >5000 nM, these are results of at least two separate experiments performed in triplicate. [b]The activation constants (K_{act} in nM) were measured in CHO cell lines expressing either vasopressin V_{1a} or V_2 or oxytocin receptor by IP-One (V_{1a} and OT-R, IP_1 accumulation) or cAMP dynamic 2 (V_2, cAMP accumulation) assays. These values are the mean ± SEM of at least three separate experiments performed in triplicate. The maximal stimulations (E_{max}) are expressed as percentages of the endogenous agonist maximal stimulation (n = 3). When there is only a weak stimulation, results are expressed as percentages of the endogenous agonist maximal stimulation at [ligand] = 1 μM (n = 2). Results are not significant (ns) when there is <10% response at [ligand] = 1 μM (n = 2). [c]The inactivation constants (K_{inact} in nM) were measured in CHO cell lines expressing either vasopressin V_{1a} or V_2 or oxytocin receptor by IP-One (V_{1a} and OT-R, inhibition of agonist-induced IP_1 accumulation) or cAMP dynamic 2 (V_2, inhibition of agonist-induced cAMP accumulation) assays. These values are the mean ± SEM of at least three separate experiments performed in triplicate. When there is only a weak inhibition, results are expressed as percentages of endogenous agonist-response inhibition at [ligand] = 1 μM (n = 2). Results are not significant (ns) when there is <10% response inhibition at [ligand] = 1 μM (n = 2). [d]n = 3. [e]n = 1. [f]n = 4. [g]n = 2.

based on the competition between free IP_1 or cAMP and IP_1-d2 or cAMP-d2 conjugate, respectively.[49] (ii) In HEK cells stably expressing V_{1a} and OT receptors, the intracellular calcium flux was determined using the fluorescent dye Indo1.

Benzazepine Series. The binding and efficacy profiles of benzoylbenzazepines **9**–**23** for the V_{1a}, V_2, and OT receptors are given in Table 2. Simple halogen substitution of the benzoyl fragment in *para* of the carboxamide link was sufficient to retain a submicromolar affinity (**9**–**11**). A two-digit nanomolar affinity was even obtained for the iodo derivative **11** on the V_{1a} receptor (K_i = 48 nM), whereas a 396 nM affinity was obtained for the OT-R. Antagonist activity was clearly observed for the V_{1a} and OT receptors, while a mixed agonist/antagonist profile was obtained on the V_2 receptor. The *n*-alkyl substituents in **12** and **13** afforded compounds with an increased potency compared to halogens. Hence the *n*-butyl analogue **13** had affinity constants of 28, 52, and 37.4 nM for the V_{1a}, V_2, and OT receptors, respectively. This is quite noticeable considering the simplicity and low molecular weight of this compound. It behaved as a relatively potent antagonist at the V_{1a} and OT receptors (K_{inact} = 421 and 113 nM, respectively) and a quite potent V_2 partial agonist (EC_{50} = 18 nM; intrinsic activity, 74% of maximum AVP induced response). The substitution by a phenyl fragment (**14**) led to a further increase in affinity with K_i of 2.28, 78, and 10.4 nM for the V_{1a}, V_2, and OR receptors, respectively. Compound **14** is a potent antagonist at the three receptor subtypes (K_{inact} = 7, 132, and 42 nM, respectively) with a preference for the V_{1a} site. The heterocyclic homologues **15** and **16** have similar

DOI: 10.1021/acs.jmedchem.8b00697
J. Med. Chem. 2018, 61, 8670−8692

Table 3. Affinity and Potency of Pyrazole Derivatives on V_{1a}, V_2, and OT Receptors

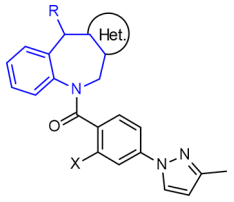

			V_{1a}-R			V_2-R			OT-R			Selectivity	
Cpd	X		affinity[a]	ago[b]	antago[c]	affinity[a]	ago[b]	antago[c]	affinity[a]	ago[b]	antago[c]	V_2/V_{1a}	V_2/OT
17	H		34±3	ns	48±8	282±11	13±4 (99±3%)	ns	84±13	ns	112±8	0.12	0.30
38	Cl		239±19	ns	535±51	38±4	16±5 (81±4%)	ns	325±48	ns	588±124	6.3	8.6
39a	H		ns[d]	ns[d]	19%[d]	>1000	ns	ns[d]	ns[d]	nd[g]	nd[g]	-	-
39b	Cl		ns	ns	ns	ns	ns	ns	ns	ns	(14±3%)	-	-
40a	H		164[d]	ns[d]	(69%)[d]	1148[d]	(68±4%)	ns	686[d]	ns	(45±18%)	0.14	0.60
40b	Cl		ns	ns	(26±1%)	100±16	28±8 (68±7%)	ns	800±75	ns	(28±14%)[f]	>100	8.0
41a	H		741[d]	ns[d]	(15%)[d]	>1000	ns	ns	1333[d]	ns	(21±14%)	<0.74	-
41b	Cl		ns	ns	ns	331±35	ns	126±33	>1000	ns	ns	>30	>3.0
42	Cl		344±14	ns	(33±3%)	50±4	9.5±3.1 (75±8%)	ns	199±84	ns	488±147	6.9	4.0
43	Cl		27±4	ns	13±3	29±5	8.4±0.4 (94±6%)	ns	17±3	ns	69±45[e]	0.93	0.59
44	Cl		ns	ns	ns	ns	ns	ns	ns	ns	ns	-	-

[a]The inhibition constants (K_i in nM) for human V_{1a}, V_2, and OT receptors were determined on CHO cell membranes by competition binding assays (displacement of radioactive [^{3}H]AVP). Results are expressed as mean ± SEM of at least three separate experiments performed in triplicate. When K_i >1000 or >5000 nM, these are results of at least two separate experiments performed in triplicate. [b]The activation constants (K_{act} in nM) were measured in CHO cell lines expressing either vasopressin V_{1a} or V_2 or oxytocin receptor by IP-One (V_{1a} and OT-R, IP_1 accumulation) or cAMP dynamic 2 (V_2, cAMP accumulation) assays. These values are the mean ± SEM of at least three separate experiments performed in triplicate. The maximal stimulations (E_{max}) are expressed as percentages of the endogenous agonist maximal stimulation (n = 3). When there is only a weak stimulation, results are expressed as percentages of the endogenous agonist maximal stimulation at [ligand] = 1 μM (n = 2). Results are not significant (ns) when there is <10% response at [ligand] = 1 μM (n = 2). [c]The inactivation constants (K_{inact} in nM) were measured in CHO cell lines expressing either vasopressin V_{1a} or V_2 or oxytocin receptor by IP-One (V_{1a} and OT-R, inhibition of agonist-induced IP_1 accumulation), or cAMP dynamic 2 (V_2, inhibition of agonist-induced cAMP accumulation) assays. These values are the mean ± SEM of at least three separate experiments performed in triplicate. When there is only a weak inhibition, results are expressed as percentages of endogenous agonist-response inhibition at [ligand] = 1 μM (n = 2). Results are not significant (ns) when there is <10% response inhibition at [ligand] = 1 μM (n = 2). [d]n = 1. [e]n = 2. [f]n = 5. [g]Not determined.

profiles with lower affinity and potency on all sites. Interestingly, the 3-methyl-pyrazolo analogue **17** recovered a high affinity at both V_{1a} (34 nM) and OT (84 nM) receptors and a lower one (282 nM) at the V_2 receptor. It showed high potency at all sites as a V_{1a}-R and OT-R antagonist (K_{inact} = 48 and 112 nM, respectively) and V_2-R full agonist (EC_{50} = 13 nM). Attempts to introduce an amino function on the benzoyl nucleus led to clear-cut changes: whereas the primary amino derivative **19** and the corresponding quaternary ammonium **21** mostly lost activity at all receptors, the intermediate dimethyl amino compound **20** showed an 82 nM affinity for the V_{1a} subtype, a 468 nM affinity for the V_2 subtype, and no affinity for the OT receptor. As most other compounds, **20** is a potent V_{1a}-R antagonist and a V_2-R agonist with potencies of 81 and 80 nM, respectively. Finally, in contrast to the inactive acetyl compound **22**, the biphenyl compound **23** was confirmed[58] as a very potent *antagonist* at the three receptor subtypes with affinities of 2.74, 0.57, and 109 nM for the V_{1a}, V_2, and OT receptors, respectively, and a marked preference for the blockade of the V_2-R mediated function (K_{inact} = 0.096 nM compared to 63 nM for V_{1a}-R and 171 nM for OT-R).

Pyrazole Series. The binding and potency profiles of pyrazole derivatives **17** and **38**−**44** for the V_{1a}, V_2, and OT receptors are given in Table 3. In this series, the substitution of the aryl linker with chlorine (compound **38**) led to a selectivity reversal compared to the unsubstituted compound **17**, with a decrease in affinity for the V_{1a} and OT receptors and an increase for the V_2 receptor. The potency profile remained unaffected, with agonism for the V_2 (EC_{50} = 16 nM) and antagonism for the two other receptor subtypes. Introduction of a keto group on the benzazepine nucleus (compounds **39a** and **39b**) resulted in a drastic loss of affinity and potency on all subtypes. This effect was less marked with the corresponding hydroxyl substitution (compound **40a** and **40b**), in particular with a chlorine substituent because **40b** showed moderate affinity (K_i = 100 nM) and a good agonist potency (EC_{50} = 28 nM) at the V_2 receptor. No agonist activity was observed for the other receptor subtypes. A similar detrimental effect was observed with an *N,N*-

DOI: 10.1021/acs.jmedchem.8b00697
J. Med. Chem. 2018, 61, 8670−8692

Table 4. Affinity and Potency of Pyrazolobenzodiazepine Derivatives on V_{1a}, V_2, and OT Receptors

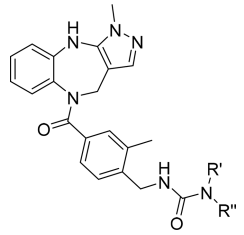

Cpd	R' N R"	V_{1a}-R			V_2-R			OT-R		
		Affinity[a]	Ago[b]	Antago[c]	Affinity[a]	Ago[b]	Antago[c]	Affinity[a]	Ago[b]	Antago[c]
Ferring	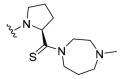	196±67	ns[d]	8±4	>1000	nd[f]	nd[f]	141	28±11 (84%)	ns[e]
WAY 267464	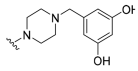	12.5±1.5	ns[d]	7±7	>1000	nd[f]	nd[f]	30.5±6.5	3±0 (40%)	ns[e]
57		1253±169	ns[d]	100±0	1666± 850	nd[f]	nd[f]	226±75	55±7 (52%)	ns[e]
58		>1000	ns[d]	95±7	>1000	nd[f]	nd[f]	>1000	300±0 (34%)	ns[e]
59	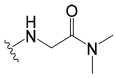	>1000	ns[d]	50±0	>1000	nd[f]	nd[f]	417	ns[d]	775± 35
60	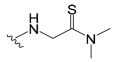	82	ns[d]	9±1	>1000	nd[f]	nd[f]	61	ns[d]	600± 0
61	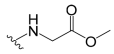	>1000	ns[d]	110±42	>1000	nd[f]	nd[f]	385	ns[d]	>1000

[a] K_i values are expressed in nM and are determined by a TR-FRET binding assay on HEK cells expressing SNAP-tagged V_{1a}, V_2, or OT receptors and incubated with a fluorescent ligand (DY647, 20 nM) with an increasing concentration of competitor. Results are expressed as mean ± SEM of one or two independent experiments. [b] EC_{50} values (intracellular calcium flux) are expressed in nM. The maximal effect is given as the percentage of the maximal response induced by OT or AVP and corresponds to mean ± SEM of two independent experiments. [c] IC_{50} (calcium flux) are expressed in nM and correspond to mean ± SEM of two independent experiments. [d] ns (nonsignificant) below 5−10% of response at 1 μM compared to the maximal response of the endogenous agonist. [e] ns (nonsignificant) below 5−10% of inhibition of the response induced by the endogenous agonist at [ligand] = 1 μM. [f] nd (not determined).

Scheme 1. Preparation of the Acid Precursors[a]

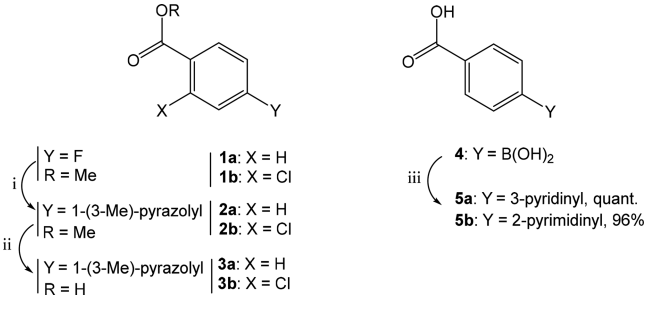

[a] Reagents and conditions: (i) 3-methylpyrazole, K_2CO_3, NMP, 120 °C, 6 h, 21−41%; (ii) HCl/H_2O, AcOH, reflux, 7 h, 96−98%; (iii) aryl bromide, $Pd(PPh_3)_4$, Na_2CO_3, H_2O, MeCN, MW 140−150 °C, 15−20 min.

dimethylamine substitution (compounds **41a** and **41b**). Interestingly, this structural modification is the only one that triggered a functional switch of the V_2 receptor from agonism to antagonism (**41b**; K_{inact} = 126 nM). Compound WAY-VNA-932 (**43**) was prepared and tested. Overall, its binding and potency profiles correspond to literature data.[60] It behaved in our hands as a moderately potent, nonspecific V_{1a} and OT receptor antagonist (K_i = 344 and 199 nM, respectively) and V_2 receptor partial agonist (K_i = 50 nM; EC_{50} = 9.5 nM with 75% of maximal response). The introduction of the Ferring and WAY-267464 pyrazolobenzodiazepine nucleus led to the potent, nonspecific ligand **43** (K_i = 27, 29, and 17 nM for the V_{1a}, V_2, and OT receptors, respectively). Again, **43** was a potent V_2-R agonist (EC_{50} = 8.4 nM) but remained antagonist at the two other receptor subtypes. Finally, removal of the aromatic component of this fragment of the molecule as in **44** led to a complete loss of activity at all receptors.

Pyrazolobenzodiazepine Series. The combination of the pyrazolobenzodiazepine nucleus with a series of homologous side chains led to compounds **57**−**61** whose pharmacological profiles are reported in Table 4. In our experimental conditions, the Ferring compound had a weak affinity for the V_{1a} and OT receptors (K_i = 196 and 141 nM, respectively) and no activity at

DOI: 10.1021/acs.jmedchem.8b00697
J. Med. Chem. 2018, 61, 8670−8692

Scheme 2. Preparation of the Unsubstituted Benzazepine 8 and Acid Coupling[a]

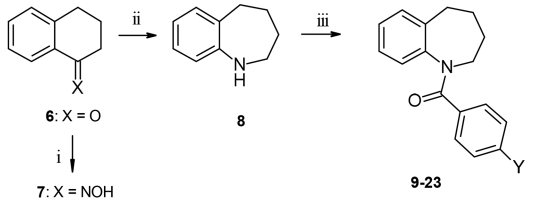

Product	Y	Yield
9	Cl	78%
10	Br	79%
11	I	38%
12	*n*Pr	86%
13	*n*Bu	83%
14	Ph	87%
15	3-pyridinyl	49%
16	2-pyrimidinyl	70%
17	1-(3-Me)-pyrazolyl	88%
18	NO_2	69%
19	NH_2	quant.[iv]
20	NMe_2	66%[v]
21	NMe_3^+	42%[vi]
22	NHAc	98%[vii]
23	NH-CO-2-biphenyl	75%[viii]

[a]Reagents and conditions: (i) $NH_2OH{\cdot}HCl$, KOH, H_2O, EtOH, 100 °C, 30 min, 92%, (ii) DIBAL-H, CH_2Cl_2, 0 °C to rt, 4 h, 73%, (iii) acyl chloride, pyridine, CH_2Cl_2, 4–20 h, (iv) **18**, H_2, Pd/C, EtOH, AcOEt, 5 h, (v) **19**, MeI, K_2CO_3, DMF, 70 °C, 6 h, (vi) **20**, MeI, $AgClO_4$, CH_2Cl_2, 2 h, (vii) **19**, Ac_2O, DIEA, CH_2Cl_2, 4 h, (viii) (a) 2-phenylbenzoic acid, $(COCl)_2$, cat. DMF, CH_2Cl_2, 2 h; (b) **19**, NEt_3, CH_2Cl_2, 0–10 °C, 2 h.

the V_2-R at micromolar concentration. We confirmed an OT-R agonist behavior with an EC_{50} = 28 nM and an 84% maximal response (based on Ca^{2+} release) compared to OT. However, this compound behaved as a potent V_{1a} receptor antagonist (Ca^{2+} release) with an IC_{50} = 8 nM. In comparison, WAY 267464 had a better affinity at both V_{1a} (K_i = 12.5 nM) and OT (K_i = 30.5 nM) receptors whereas no activity was measured at the V_2 receptor. This compound is an equipotent V_{1a}-R antagonist compared to the Ferring compound (EC_{50} = 7 nM) and a potent OT-R agonist (EC_{50} = 3 nM). However, the maximal response obtained in our experimental conditions is limited to 40% of the maximal response obtained with OT. Hence, the gain in affinity is balanced by a loss in potency due to partial agonism. The compound **57** had lower affinity on all receptor subtypes with a preference for the OT-R (K_i = 226 nM). Very interestingly, **57** remains an agonist with a high potency (EC_{50} = 55 nM) and an increased intrinsic activity compared to WAY 267464 (52% instead of 40% of the maximal response). The functional selectivity of **57** versus the V_{1a}-R is also reversed compared to the Ferring compound because there was a moderate (2-fold) preference for the OT-R. A very low affinity was detected at the V_2 receptor (K_i = 1666 nM). The carboxamide analogue **58** of the thiocarboxamide **57** had a parallel profile but was much less potent. Remarkably, the three open chain analogues **59**–**61** retained some activity but switched to low affinity OT-R *antagonists*. Despite its small size and its relative flexibility, the thiocarboxamide **60** was actually a rather potent (IC_{50} = 9 nM) and specific V_{1a} receptor antagonist based on functional assays because it was 60-fold less potent as an OT-R antagonist and showed no affinity for the V_2 subtype up to 1 μM concentration.

Signaling Profile of Compound 57 in Vitro. On the basis of previous screening data and predictive bioavailability characteristics (see below), we focused on our best candidate, compound **57**, and further studied its pharmacological profile by assessing its effects on calcium release and β-arrestin2 recruitment in HEK293FT cell lines transiently expressing human OT, V_{1a}, V_{1b}, or V_2 receptors with either aequorin sensor or β-arrestin2 for calcium or BRET1 recruitment assays, respectively. This activity was compared to those of several reference molecules: oxytocin and carbetocin as full and biased peptide agonists, respectively, and WAY-267464 as nonpeptide partial agonist (Figure 1 and Table 5).

Regarding calcium release (Figure 1A and Table 5), oxytocin was the most potent agonist on OT-R; carbetocin, WAY-267464, and compound **57** had similar potencies (EC_{50} = 25 nM), with compound **57** showing the best maximal effect (E_{max} = 96%). We compared these four compounds on mouse OT-R calcium release prior to in vivo testing in mice. Oxytocin was the most potent agonist, and compound **57** showed better potency (EC_{50} = 18 nM) and maximal effect (E_{max} = 96%) than carbetocin and WAY-267464 (Supporting Information, Figure S1A and Table 5). Now focusing on β-arrestin recruitment (Figure 1B and Table 5), carbetocin retained a high potency (EC_{50} = 10 nM) however with a partial maximal response (E_{max} = 42%); WAY-267464 showed a 6-fold lower potency compared to that measured for calcium release, suggesting a potential bias in its signaling. Compound **57** retained high potency (EC_{50} = 62 nM) and maximal response (E_{max} = 77%). Thus, compound **57** was the most potent agonist behind oxytocin to recruit β-arrestin. Furthermore, we tested the specificity of previous compounds by measuring their effects on V_{1a}, V_{1b}, and V_2 vasopressin receptor-mediated activation of calcium release and β-arrestin recruitment (Figure 1C–H and Table 5). Carbetocin poorly activated V_{1b}-R and V_2-R without effect on V_{1a}-R-induced calcium release. It had no effect on β-arrestin recruitment mediated by V_{1a}-R and V_{1b}-R and a very small effect on V_2-R mediated arrestin release (E_{max} = 8% at micromolar concentration). WAY-267464 activated partially V_2-R mediated calcium release (EC_{50} = 2300 nM; E_{max} = 43%) and had no effect on AVP induced arrestin release on the three receptor subtypes. WAY-267464 is also known to antagonize V_{1a} receptors.[51] We thus tested whether **57** would similarly block the effects of vasopressin on V_{1a} and V_{1b} receptors. We found that compound **57** poorly antagonized vasopressin induced calcium release on V_{1a}-R (IC_{50} = 5900 nM) and was devoid of effect on V_{1b}-R (Supporting Information, Figure S1B,C). However, compound **57** significantly activated V_2 receptors as measured on both pathways. Finally, we tested the effects of the Pfizer OT-R antagonist PF 3274167[72] on the activation of OT and V_2 receptors by compound **57**. PF3274167 totally suppressed and partially reduced the effects of **57** on OT-R and V_2-R, respectively (Table 5; Supporting Information, Figure S1D,E). In conclusion, compound **57** acts as a nonbiased agonist on OT-R with the most potent and specific effects among tested synthetic compounds.

Biological Activity of Compound 57 in Vivo: Effects in a Mouse Model of ASD (Figure 2). Mice lacking the mu opioid receptor ($Oprm1^{-/-}$) recapitulate all core symptoms of ASD: deficient social interaction and altered communication together with stereotyped behaviors; they also display multiple comorbid symptoms of ASD such as exacerbated anxiety and

DOI: 10.1021/acs.jmedchem.8b00697
J. Med. Chem. 2018, 61, 8670–8692

Scheme 3. Synthesis of Cyclic Amines Used[a]

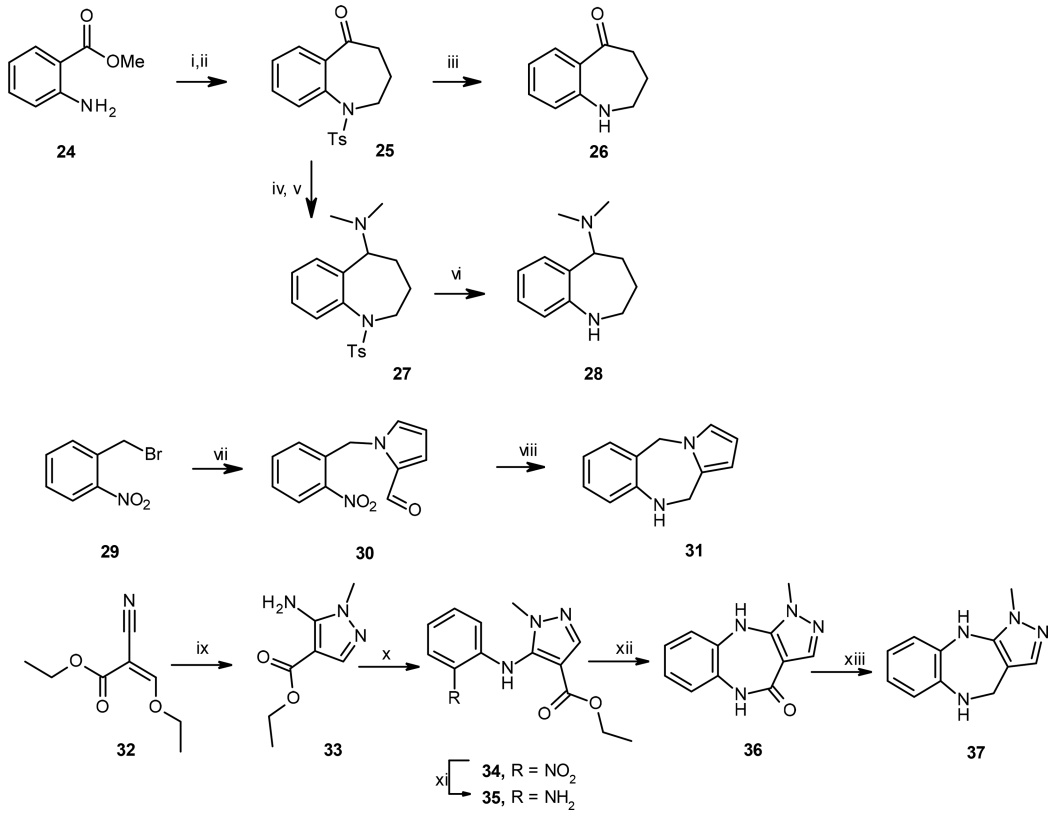

[a]Reagents and conditions: (i) TsCl, pyridine, 0 °C, 1 h, 98%; (ii) (a) NaH, $Br(CH_2)_3COOEt$, DMF, 14 h, rt, then 90 °C, 6 h, (b) NaH, MeOH/toluene 17 h, (c) AcOH, HCl, EtOH, H_2O, 100 °C, 8 h, 62%; (iii) PPA, 110 °C, 2 h, quant; (iv) (a) $MeNH_2$, MeOH, MW 130 °C, 8 min, (b) $NaBH_4$, 1 h, 98%; (v) HCHO, $NaBH_3CN$, AcOH, MeOH, 2 h, 90%; (vi) PPA, 120 °C, 2 h, quant; (vii) pyrrole-2-carboxaldehyde, NaH, DMF, 4 h, quant; (viii) H_2, Pd/C, EtOH, 60 psi, 3 h, 70%; (ix) $MeNHNH_2$, EtOH, reflux, 17 h, 92%; (x) NaH, 2-fluoronitrobenzene, THF, 48 h, 78%; (xi) H_2, Pd/C, EtOH, AcOEt, 1 h, 99%; (xii) AcOH/*i*PrOH 1:9, 160 °C, 48 h, 89%; (xiii) $LiAlH_4$, THF, reflux, 44 h, 86%.

increased sensitivity to seizures.[73−75] They thus demonstrate remarkable face validity as a mouse model of ASD. Interestingly, these animals also display alterations in the oxytocin/vasopressin system, as evidenced by reduced number of oxytocin transcripts in the nucleus accumbens,[73] a key structure for social reward,[76] and consistent increase in OT-R binding in this same region as well as in the amygdala.[77] Here we reasoned that stimulating OT receptors using the promising OT-R agonist compound **57** should relieve social interaction deficits in *Oprm1*$^{-/-}$ animals. To challenge this hypothesis, we administered an acute intraperitoneal injection of vehicle or **57** (at 10 or 20 mg/kg) to *Oprm1*$^{+/+}$ or *Oprm1*$^{-/-}$ unfamiliar (non cagemates, same age, same sex, and same treatment) mice before introducing them by pairs in an open-field for 10 min testing. Behavioral parameters were scored on video recordings to assess the quality of social interactions in these animals, namely the number of nose contacts (NCs), the time spent in NC, the mean duration of NCs, the number of following episodes, and the number of grooming episodes occurring after a social contact, an index of social avoidance.[73] At the dose of 10 mg/kg (Figure 2), **57** restored the number of NCs (genotype effect, $F_{1,42} = 54.2$, $p < 0.0001$; dose effect, $F_{2,42} = 9.6$, $p < 0.001$; genotype × dose interaction, $F_{2,42} = 16.8$, $p < 0.0001$) and time spent in NC (genotype, $F_{1,42} = 45.6$, $p < 0.0001$; dose, $F_{2,42} = 19.9$, $p < 0.0001$; genotype × dose: $F_{2,42} = 17.4$, $p < 0.0001$), the mean duration of NC (genotype, $F_{1,42} = 15.1$, $p < 0.001$; dose, $F_{2,42} = 19.5$, $p < 0.0001$; genotype × dose, $F_{2,42} = 19.8$, $p < 0.0001$) and the number of following episodes (genotype, $F_{1,42} = 38.9$, $p < 0.001$; dose, $F_{2,42} = 24.4$, $p < 0.0001$; genotype × dose, $F_{2,42} = 4.2$, $p < 0.05$) measured in *Oprm1*$^{-/-}$ mice to similar levels as measured in wild-type controls. Moreover, at this dose, **57** also suppressed grooming episodes occurring after a social contact in mutants (genotype, $F_{1,42} = 8.5$, $p < 0.01$; dose, $F_{2,42} = 11.3$, $p < 0.001$; genotype × dose, $F_{2,42} = 21.4$, $p < 0.0001$). The OT-R agonist had no effect in *Oprm1*$^{+/+}$ mice at this dose, except that it increased the number of following episodes. At the dose of 20 mg/kg, compound **57** demonstrated less significant beneficial effects on social parameters measured in mutant animals and started to show some detrimental effects on these parameters in wild-type controls (Figure 2A−E). Such effects may have resulted either from excessive OT-R activation or from recruitment/blockade of V_{1a} or V_{1b} vasopressin receptors at high doses, peripherally or centrally. To our knowledge, our results are the first evidence that a nonpeptidic OT-R compound can alleviate core symptoms in the context of ASD.

The actual presence in the mouse brain of compound **57** after a 10 mg/kg ip administration has been determined by showing an experimental brain exposure of 399 ± 104 min.ng/g.

DISCUSSION

Our ultimate goal is the design and development of drugs improving life of patients with autism spectrum disorders. As discussed in the Introduction, the oxytocin receptor appears as a valid target because OT has already shown beneficial effects in

DOI: 10.1021/acs.jmedchem.8b00697
J. Med. Chem. 2018, 61, 8670−8692

Scheme 4. Coupling of the Different Amines with Acids 3a and 3b

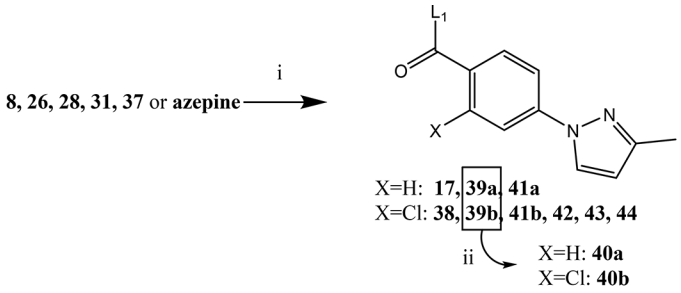

[a] Reagents and conditions: (i) (a) **3a** or **3b**, $SOCl_2$, cat. NMP, CH_2Cl_2, overnight, (b) **8**, **26**, **28**, **31**, **37** or azepine, pyridine, CH_2Cl_2, 4-20 h (**43**: MW 80 °C, 8 min), 17-88%; (ii) $NaBH_4$, MeOH, 2 h, 73-95%.

Compound	Amine (L_1)	Acid	Yield	Compound	Amine (L_1)	Acid	Yield
17	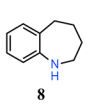 **8**	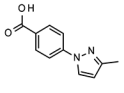 **3a**	88%	**38** (*Otsuka*)	 **8**	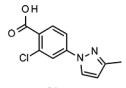 **3b**	61%
39a	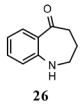 **26**	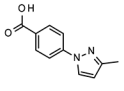 **3a**	32%	**39b**	 **26**	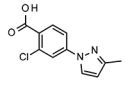 **3b**	30%
40a		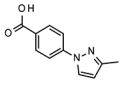 **3a**	73%[iii]	**40b**		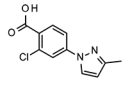 **3b**	95%[iii]
41a	 **28**	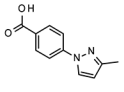 **3a**	70%	**41b**	 **28**	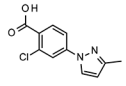 **3b**	17%
42 VNA-932	 **31**	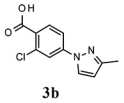 **3b**	43%	**43**	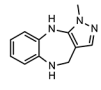 **37**	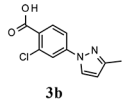 **3b**	81%
44		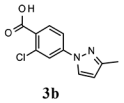 **3b**	35%				

Scheme 5. Preparation of Proline Derivatives 45−49[a]

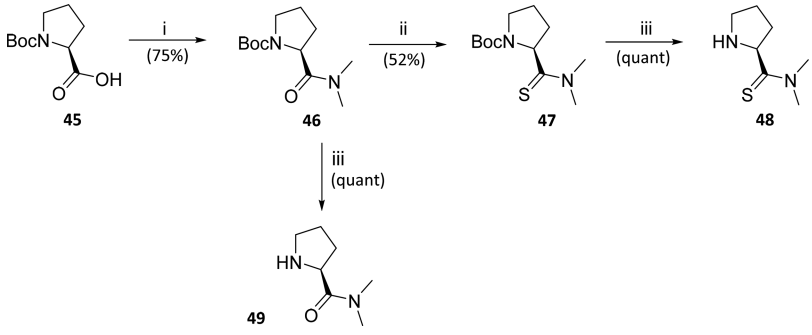

[a]Reagents and conditions: (i) EDCI, HOBt, Et_3N, NMe_2, CH_2Cl_2, overnight; (ii) Lawesson reagent, toluene, overnight, 70 °C; (iii) TFA/CH_2Cl_2 (1/1, v/v), 30 min.

human after i.n. administration.[15−36] However, OT is not metabolically stable, poorly penetrates the brain, even after intranasal administration, and its development as a marketed drug to treat ASD is hampered by intellectual property

DOI: 10.1021/acs.jmedchem.8b00697
J. Med. Chem. 2018, 61, 8670−8692

Scheme 6. Preparation of Fragments 52−54[a]

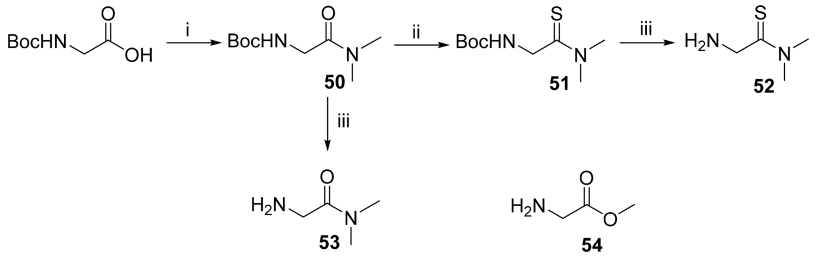

[a]Reagents and conditions: (i) EDCI, HOBt, Et_3N, NMe_2, CH_2Cl_2, overnight, 46%; (ii) Lawesson reagent, toluene, overnight, 70 °C, 63%; (iii) TFA/CH_2Cl_2 (1/1, 30 min), quant.

Scheme 7. Synthesis of Compounds 57−61[a]

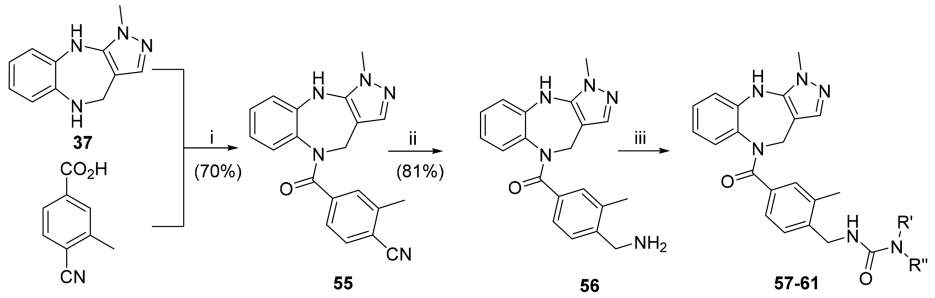

(i) (a) $(COCl)_2$, DMF cat., CH_2Cl_2, 2 h; (b) Et_3N, CH_2Cl_2, overnight ; (ii) $NaBH_4$, $CoCl_2.6H_2O$, MeOH, 1 h; (iii) (a) compounds **48, 49 or 52-54**, CDI, DIEA, DMF, overnight, 41-67%.

Compound	Amine -NR'R''	Yield (%)	Compound	Amine -NR'R''	Yield (%)
57		41	**59**	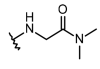	65
58		66	**60**		67
			61		66

[a](i) (a) $(COCl)_2$, DMF cat., CH_2Cl_2, 2 h, (b) Et_3N, CH_2Cl_2, overnight; (ii) $NaBH_4$, $CoCl_2.6H_2O$, MeOH, 1 h; (iii) (a) compounds **48**, **49**, or **52−54**, CDI, DIEA, DMF, overnight, 41−67%.

considerations. Consequently, our aim was to design and develop a novel nonpeptide OT-R agonist active in animal models of autism after peripheral administration. To our knowledge, no compound with such a profile has been disclosed yet.

From the first SAR run (Table 2), we concluded that the benzoylbenzazepine pharmacophore is indeed relevant to generate ligands with high affinity at the vasopressin/oxytocin receptors. Very minimal substitution, such as a halogen (**11**), an alkyl (**13**), a heterocycle (**17**), or an amine (**20**), are sufficient to afford two-digit nanomolar ligands at one or several receptor subtypes. It was encouraging to observe that minor structural changes afforded high affinity V_2-R ligands with functional profiles ranging from full antagonist (**23**) to full agonist (**17**). Hence, as expected, replacement of the bulky and hydrophobic aromatic biphenyl fragment of the potent, nonspecific antagonist **23** by a smaller, more hydrophilic 3-methyl-pyrazole fragment led to a V_2-R full agonist (compound **17**). It was, however, disappointing to observe that such a shift could not be obtained on the V_{1a}-R or OT-R where the compound remained an antagonist despite the very high sequence homology and structural similarity of the vasopressin/oxytocin binding sites. This illustrates one more time the subtlety of ligand−receptor interaction and activation in this receptor family.[49]

Because the 3-methyl-pyrazole derivative **17** of the benzoylbenzazepine pharmacophore was the only compound showing full agonist activity at a vasopressin/oxytocin receptor (V_2 subtype), we decided to pursue our quest for an OT-R agonist around the 3-methyl-1-pyrazoloaryl pharmacophore in replacing the benzazepine fragment by other nuclei derived from reference ligands. The central aryl linker was bare or substituted with chlorine in position 2. The binding and functional profiles of these hybrid molecules are reported in Table 3. Taken together, the results confirm that it is indeed possible to modulate the affinity and selectivity profile of vasopressin/oxytocin ligands in playing with the benzazepine component of

DOI: 10.1021/acs.jmedchem.8b00697
J. Med. Chem. 2018, 61, 8670−8692

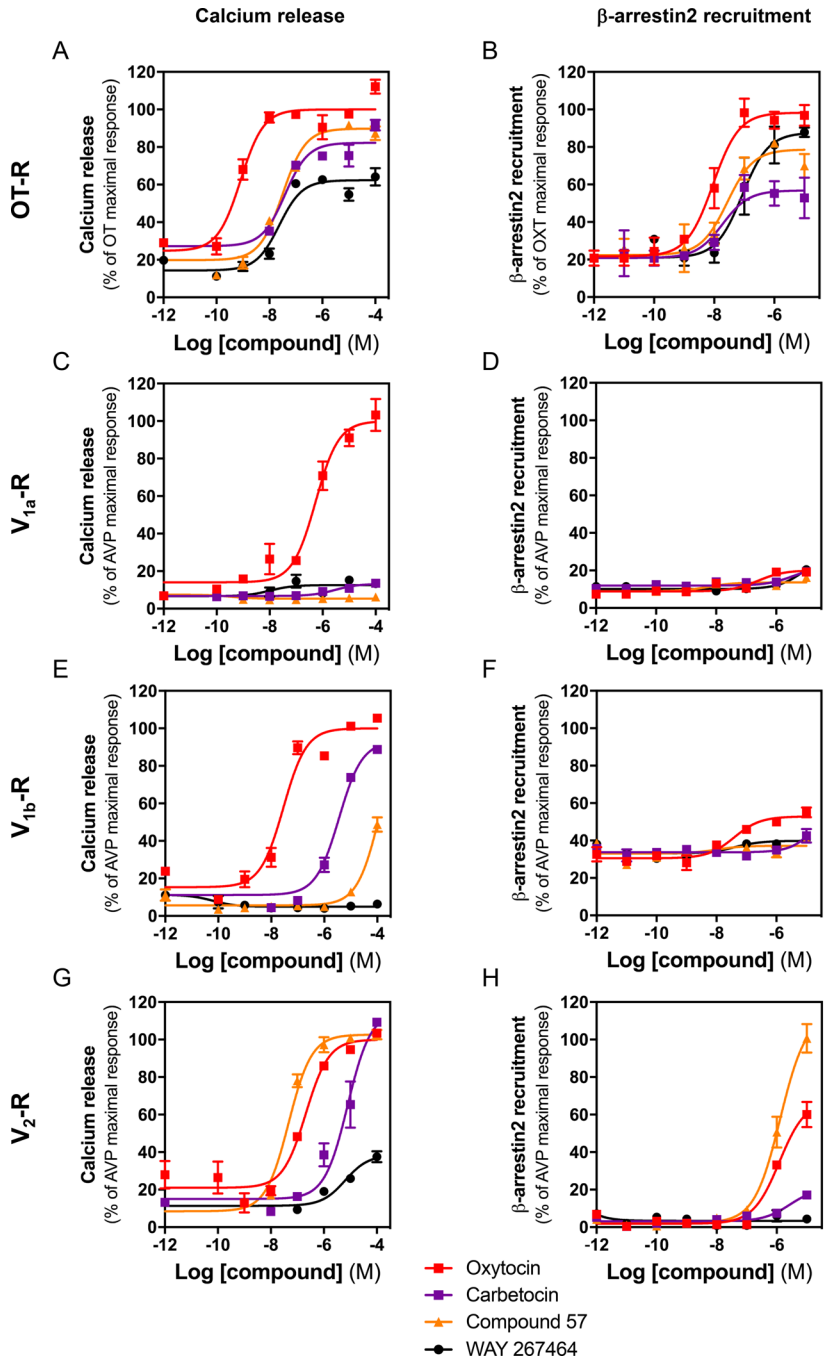

Figure 1. Pharmacological profile of OTR agonists, oxytocin, compound **57**, carbetocin, and WAY-267464, on oxytocin and vasopressin receptors. Representative dose−responses from three to four experiments of oxytocin (red), compound **57** (orange), carbetocin (purple), and WAY-267464 (black) on OT (A,B), V_{1a} (C,D), V_{1b} (E,F), and V_2 (G,H) receptors are presented on the two major signaling pathways of these receptors, calcium release (A,C,E,G), and *β*-arrestin2 recruitment (B,D,F,H). Oxytocin appears as the most potent agonist on OTR to activate calcium release; carbetocin, WAY-267464, and compound **57** have similar affinities, with compound **57** showing the best maximal effect. Regarding *β*-arrestin recruitment, carbetocin acts as a partial agonist and WAY-267464 shows lower affinity compared to that measured for calcium release, suggesting a bias in its signaling.

the ligands. Hybrid molecules with the aryl-1-(3-methyl)-pyrazole pharmacophore remained in most cases agonists at the V_2-R, however, they did not switch to agonists neither at the V_{1a} receptor nor at the target OT receptor. It thus appeared from this study and from our previous work[49] that the only entry to OT agonism is the pyrazolobenzodiazepine synthon as in Ferring and Wyeth WAY-267464 compounds.

Very limited SAR studies were reported around the Ferring compound. In the initial disclosure,[48] its functional potency using a reporter gene assay on OT-R and V_2-R was reported (EC_{50} = 33 and 850 nM, respectively). Affinity data as well as its extended functional profile were published later, together with a troncature study and the profiling of few hybrid molecules.[49] To our knowledge, only one SAR study was published around WAY-267464, dealing with flexible analogues that turned from OT-R agonists to V1a-R antagonists, confirming the high sensitivity of the system.[78] Our own SAR study around the pyrazolobenzodiazepine reported here (Table 4) led to the

DOI: 10.1021/acs.jmedchem.8b00697
J. Med. Chem. 2018, 61, 8670−8692

Table 5. Affinity and Potency of OTR Agonists Compound 57, Carbetocin, and WAY-267464 on Calcium Release and β-Arrestin Recruitment on Oxytocin and Vasopressin Receptors[a]

		oxytocin	carbetocin	compd **57**		PF3274167	WAY-267464
		agonist	agonist	agonist	antagonist (AVP 2 nM)	antagonist on compd **57**	agonist
calcium	hOTR	0.7 ± 0.3 (100)	41 ± 17 (83 ± 20)	25 ± 7 (96 ± 8)	nd	600 ± 300	24 ± 12 (70 ± 4)
	mOTR	2.0 ± 0.4 (100)	62 ± 31 (85 ± 4)	18 ± 8 (95 ± 4)	nd	nd	78 ± 25 (86 ± 2)
	$V_{1a}R$	260 ± 130 (100)	ns	ns	5900 ± 2700	nd	ns
	$V_{1b}R$	39 ± 7 (100)	27000 ± 17000 (75 ± 8)	ns	ns	nd	ns
	V_2R	210 ± 40 (100)	6700 ± 2700 (103 ± 7)	41 ± 4 (101 ± 4)	nd	1530 ± 550	2300 ± 2000 (43 ± 9)
		agonist	agonist	agonist	antagonist (AVP 100 nM)	antagonist on compd **57**	agonist
β-arrestin	OTR	26 ± 15 (100)	10 ± 6 (42 ± 7)	62 ± 43 (77 ± 11)	nd	63 ± 42	150 ± 60 (84 ± 5)
	$V_{1a}R$	ns	ns	ns	2200 ± 200	nd	ns
	$V_{1b}R$	29 ± 14 (49 ± 12)	ns	ns	ns	nd	ns
	V_2R	810 ± 250 (69 ± 18)	1100 ± 600 (8 ± 2)	660 ± 220 (97 ± 4)	nd	2620 ± 1260	ns

[a]EC_{50} ("agonist") or IC_{50} ("antagonist") and E_{max} values are expressed respectively in nM and as the percentage of the maximal response induced by OT or AVP. The values were measured in HEK293FT cell lines expressing transiently human OT, mouse OT, V_{1a}, V_{1b}, or V_2 receptors with either aequorin sensor or β-arrestin2 for calcium or BRET1 recruitment assays, respectively. These values are the mean ± SEM of at least three to four separate experiments performed in triplicate per receptor and per compound. ns: nonsignificant (no value measured). nd: not determined.

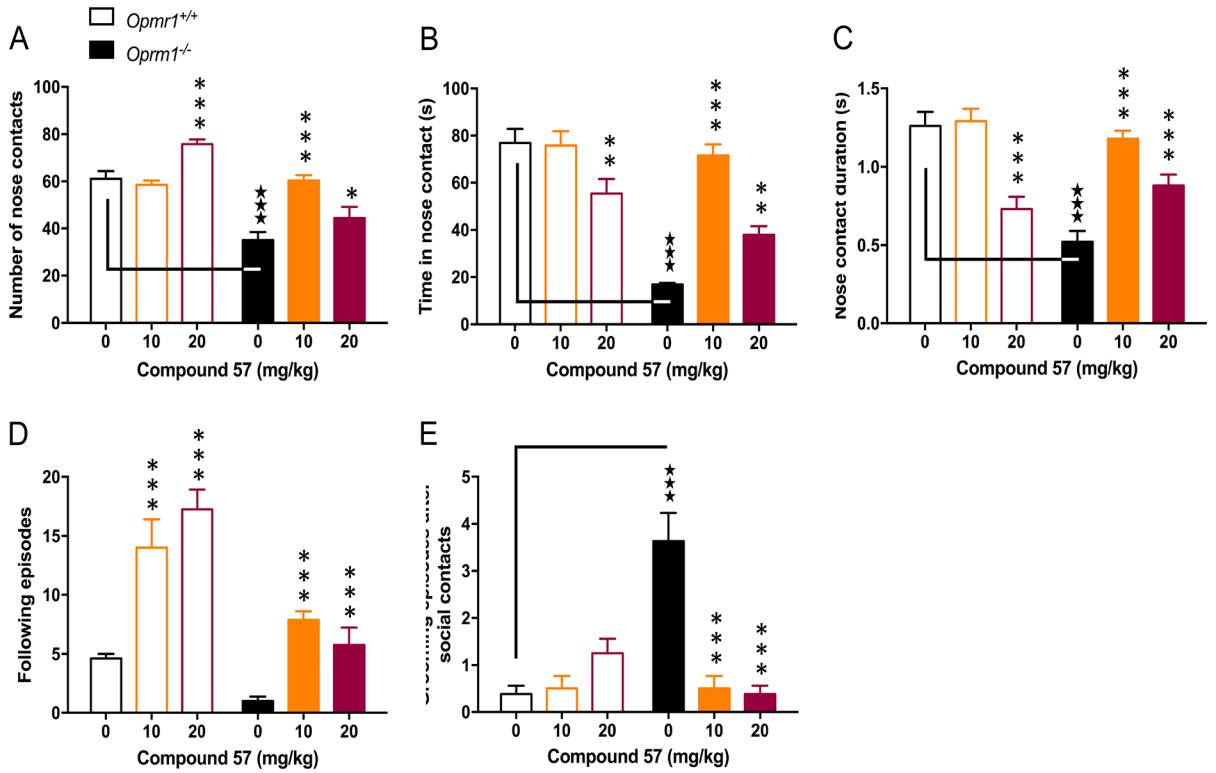

Figure 2. Compound **57** restores social interaction in *Oprm1*$^{-/-}$ mice. In the direct social interaction test, an acute administration of compound **57** (ip; 10 or 20 mg/kg) increases the number of nose contacts (NCs), the time spent in NC, duration of NC, and number of following episodes in *Oprm1*$^{-/-}$ mice while it decreases the number of grooming episodes occurring after a social contact. Compound **57** at a moderate dose (10 mg/kg) fully restores these social parameters to *Oprm1*$^{+/+}$ levels, whereas at a higher dose (20 mg/kg) this beneficial outcome is less significant and detrimental effects start to be observed in wild-type controls. Data are presented as mean ± SEM ($n = 8$ per genotype and treatment). Solid stars: comparison to vehicle-treated *Oprm1*$^{+/+}$ mice. Asterisks: comparison to vehicle-treated animals of the same genotype (two-way ANOVA followed by Newman−Keules posthoc test). One symbo,: $p < 0.05$; two symbols, $p < 0.01$; three symbols, $p < 0.001$.

discovery of a new potent agonist, compound **57**, that shows lower molecular weight, better selectivity versus the V_{1a} receptor, similar EC_{50}, and improved efficacy (52%−96%) compared to Ferring compound or WAY-267464. However, we found difficult to conclude to a superiority of **57** based on in vitro affinity or simple potency and intrinsic activity measurements. Indeed, in our experience, such data are very much dependent on the experimental conditions (cells, expression vectors, stable or transient expression, receptor density, and environment, assay, experimenter, etc.). As an illustration, we report in Table 6 binding and potency data for OT, Ferring compound, WAY-267464, and compound **57** collected from literature and from our own experiments. As can be observed, affinity data are usually consistent but may vary significantly. For

DOI: 10.1021/acs.jmedchem.8b00697
J. Med. Chem. 2018, 61, 8670−8692

Table 6. Binding Profiles and Potency Evaluation at OT-R of Reference Compounds and Compound 57 in Different Experimental Conditions

		affinity (K_i; nM ± SD)			efficacy at OT-R	
compd	experimental conditions	V_{1a}-R	V_2-R	OT-R	EC_{50} (nM ± SD)	maximal response (%)
OT	IP1 (CHO; stable)[49]				10.6 ± 0.3	100
	gene reporter (CHO; transient)				0.18 ± 0.07 (n = 20)	100
Ferring	radioligand binding (CHO)[49]	330 ± 38	>1000	147 ± 11		
	FRET binding (HEK)	196 ± 67	>1000	28 ± 11		
	IP1 (CHO; stable)[49]				667 ± 68 (n = 3)	58 ± 2 (n = 3)
	gene reporter[48] (CHO; transient)				33 ± 15 ($n \geq 3$)	100 ($n \geq 3$)
WAY-267464	radioligand binding[40] (CHO; stable)	>5800	>5800	58.4 ± 11.3		
	radioligand binding[78] (HEK; membranes)	27 ± 3	nd	230 ± 31		
	radioligand binding[51] (HEK; membranes)	113 ± 32	nd	978 ± 71		
	FRET binding (HEK; stable)	12.5 ± 1.5	>1000	30.5 ± 6.5		
	calcium[40] (CHO; stable)				61.3 ± 4.5	87.1 ± 0.9
	IP1[78] (HEK; stable)				420 ± 59	nd
	calcium[51] (HEK; stable)				881 ± 383	nd
	calcium (HEK; stable)				3 ± 0	40
57	calcium (HEK; stable)				55 ± 7	52
	calcium (HEK; transient)				25 ± 7	96 ± 8

Table 7. Calculated Physicochemical Characteristics of Reference and Compound 57

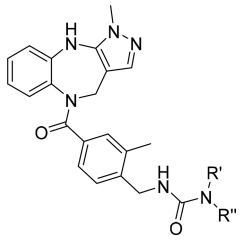

Compound		MW (g/mol)	Calc. LogD (pH =7.4)[80]	Calc. LogP[80]	PSA (Å)[80]	LogBB[79,80]
Ferring	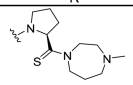	600.78	1.33	2.74	90.18	-1.04
WAY-267464	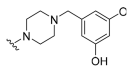	581.66	2.69	2.71	127.40	-1.41
57 (LIT-001)		531.67	2.84	2.84	85.74	-0.75

example, K_i varies from 12.5 to 113 nM[40,49,51] to more than 5800 nM[48] for the reference WAY-267464. As expected, more drastic differences are observed for potency. Hence EC_{50} may vary for the same compound from 33 to 667 nM (Ferring compound), from 3 nM to 881 nM (WAY-267464), or from 16 to 55 nM (**57**) according to differences in systems of expression or in quantification assays. Important variations are also observed in the achievable maximal responses. For instance, for the Ferring compound, maximal efficacy varies from 58% to 84% and ultimately 100% in moving from an IP1, to a Ca^{2+} and to a gene reporter assay in CHO cells, respectively, which might be understood because different levels of amplification are involved. However, in looking at the Ca^{2+} signal in HEK cells, the Ferring compound behaved mainly as a full agonist (EC_{50} = 111−149 nM; 88−100% maximal response). The reverse trend is observed for the widely used OT-R "agonist" WAY-267464 compound which displayed maximal responses varying from 87% (CHO/Ca^{2+}) to 27% (HEK/Ca^{2+}). As can be seen from Tables 4 and 6, compound **57** behaved as a partial agonist in one series of experiment (52%; HEK/Ca^{2+}) and a full agonist in another series (96%; transient HEK/Ca^{2+}).

As reported above, variations in measurements of in vitro affinity, potency, and intrinsic activity profiles of pharmacological probes may lead to misinterpretation of in vivo data. In particular, WAY-267464 was used as a specific nonpeptide OT agonist in several studies,[40,50] while it has clearly been

DOI: 10.1021/acs.jmedchem.8b00697
J. Med. Chem. 2018, 61, 8670−8692

demonstrated more recently that some of its in vivo pharmacological functions are mainly driven by its V_{1a} antagonist activity.[51] The correspondence between diverse in vitro and in vivo data is not straightforward, and this led us to evaluate the signaling profile and the efficacy of one of our new compounds in animal models of the target disease. The selection criteria of the molecule to be further tested in vitro and in vivo were a combination of its in vitro activity and its putative ability to penetrate the brain. Some appropriate physicochemical parameters of the best candidates were calculated[79,80] (Table 7). Compound **57** has a molecular weight slightly lower than the reference WAY-267464, which may favor passive absorption. Its thermodynamic solubility in buffer at pH 7.4 is fair: 0.68 ± 0.07 mM (WAY-267464, 5 mM). Its calculated log *D* is in the perfect range for brain penetration (log *D* = 2.84; experimental log *D* = 2.0 ± 0.3 at pH = 7.4). The polar surface area is also more favorable, which leads to a logBB value (log BB = 0.133 − 0.0153PSA + 0.1522log *P*) above the target threshold (log BB = −1) to optimize brain penetration.[80] On this basis, compound **57** (named **LIT-001**) was selected for a more detailed signaling study (Table 5, Figure 1 and Supporting Information, Figure S1) and for in vivo studies (Figure 2).

In vitro signaling experiments allowed us to identify compound **57** as a nonbiased OT-R agonist on the two main signaling pathways of this receptor, with minor antagonist effect on V_{1a} and agonist effect on V_{1b} receptors, observed at high concentrations only (Table 5 and Figure 1). Compound **57**, however, activated V_2-R, which is not likely to impact social behavior as V_2-R are not expressed in the central nervous system[81,82] but may cause fluid retention.[83] This agonist effect was similar to the effect of oxytocin, which was shown to be safe for chronic use in patients.[84] In comparison, the reference molecule WAY-267464, in our experimental setup, had only partial effects or lower affinity to stimulate OT-R-mediated signaling. WAY-267464, as compound **57**, antagonizes V_{1a}-R, an effect that may contribute to facilitate social interaction.[85] We could not evidence G protein-biased agonism of carbetocin on OT-R, as previously shown,[86] but such bias was very clear on V_{1b} and V_2 receptors. Finally, oxytocin bound and activated OT-R as well as V_{1a}, V_{1b}, and V_2 receptors, as previously demonstrated.[87] Thus, compound **57** clearly appeared as the most promising alternative to oxytocin for therapeutic development as a potent nonpeptidic OT-R agonist, with potential selectivity in the CNS after peripheral administration.

Consistent with this, **57** efficiently relieved social interaction deficits in *Oprm1*$^{-/-}$ mice, a mouse model of autism,[73] by normalizing the number and duration of nose contacts, the frequency of following episodes and the occurrence of grooming episodes after a social contact to wild-type levels at the dose of 10 mg/kg (Figure 2). These effects were observed following systemic (intraperitoneal) administration that led to a measured brain concentration of compound **57** in the range of its K_i (399 min·ng/g at 10 mg/kg ip). A full pharmacokinetic study remains to be done but these preliminary results suggest brain penetrance and bioavailability for this OT-R agonist, while oxytocin is known as poorly brain penetrant (except through i.n. route) and highly sensitive to peripheral degradation.

CONCLUSION

An extended structure−activity relationship study around vasopressin/oxytocin nonpeptide pharmacophores further illustrated[49] the subtlety of the activation mechanisms of the V_{1a}, V_{1b}, V_2, and OT receptors. Minor structural changes affect significantly the affinity and selectivity profiles of ligands in spite of the high structural similarity of the binding clefts of the members of this GPCR subgroup. In this context, finding OT-R nonpeptide agonists represented a challenge. Our study led to the discovery of **LIT-001** (compound **57**) that represents the first nonpeptide OT receptor agonist active in an animal model of ASD after peripheral ip administration. As a proof of concept, **LIT-001** is a useful pharmacological tool to explore the implication of oxytocin in social attachment behaviors and it may pave the way to the development of optimized preclinical candidates to treat some components of autism.

EXPERIMENTAL SECTION

Chemistry. *General Methods.* General methods are as described in ref 49. Purity (≥95% for all compounds) was determined by analytical HPLC in the same conditions as previously reported.[49] Elementary analysis of the final compounds have been determined by the Service Central d'Analyse of the Centre National de la Recherche Scientifique (CNRS; Vernaison) or by the core service of microanalysis of the Institute of Chemistry, Strasbourg University.

The synthesis of precursor compounds **1**−**8**, **28**, **31**, and **37** is reported and available in the Supporting Information.

General Method A for the Coupling of Amines and Benzoic Acids. To a solution of benzoic acids (1.1 equiv) in anhydrous CH_2Cl_2 under argon were added 2−3 drops of NMP and 1.2 equiv of $SOCl_2$. The mixture was stirred overnight at rt and evaporated. The residue was dissolved in anhydrous CH_2Cl_2 and added dropwise at 0 °C under argon to a mixture of the amine (1.0 equiv) and anhydrous pyridine (5.0 equiv) in anhydrous CH_2Cl_2. The mixture was stirred 30 min at 0 °C and then at rt for 4−20 h. The mixture was then poured into water and extracted with CH_2Cl_2. The aqueous phase was washed with 1 N HCl and saturated aqueous K_2CO_3, dried over Na_2SO_4, and evaporated. The residue was purified by chromatography on a silica gel column (heptane → AcOEt excepted AcOEt → AcOEt/MeOH 9:1 for **41a**,**b**).

*1-(4-Chlorobenzoyl)-2,3,4,5-tetrahydro-1H-1-benzazepine (**9**).* Benzazepine **8** reacted with 4-chlorobenzoic acid according to general method A to give **9** as a white solid (yield 78%). R_f = 0.4 (hept/AcOEt 7/3). MP = 84 °C. ^{1}H NMR (300 MHz, $CDCl_3$): δ 1.40−1.60 (m, 1H), 1.90−2.18 (m, 3H), 2.70−3.10 (m, 3H), 5.00 (dl app, 1H, *J* = 13.4 Hz), 6.62 (d, 1H, *J* = 7.8 Hz), 6.93 (t, 1H, *J* = 7.2 Hz), 7.03−7.18 (m, 5H), 7.23 (d, 1H, *J* = 6.8 Hz). ^{13}C NMR (75 MHz, $CDCl_3$): δ 26.2, 29.6, 35.0, 47.7, 127.1, 127.3, 127.9, 128.2, 129.6, 130.1, 134.6, 135.5, 139.2, 143.7, 167.9. IR (ATR): λ (cm^{-1}) 2940, 2918, 1644, 1592, 1576, 1488, 1434, 1398, 1376, 1359, 1306, 1273, 1258, 1174, 1137, 1092, 1071, 1012, 960, 917, 852, 841, 823, 766, 751, 745, 724, 692, 574, 555, 540. HRMS (ES) *m*/*z* calcd for $C_{17}H_{16}ClNO$ $[M + Na]^+$ 308.0813, found 308.0819. HPLC t_R = 20.7 min, purity 98.8% (254 nm).

*1-(4-Bromobenzoyl)-2,3,4,5-tetrahydro-1H-1-benzazepine (**10**).* Benzazepine **8** reacted with 4-bromobenzoic acid according to general method A to give **10** as a white solid (yield 79%). R_f = 0.5 (hept/AcOEt 7/3). MP = 102 °C. ^{1}H NMR (300 MHz, $CDCl_3$): δ 1.40−1.60 (m, 1H), 1.87−2.20 (m, 3H), 2.70−3.10 (m, 3H), 5.00 (dl app, 1H, *J* = 13.1 Hz), 6.62 (d, 1H, *J* = 7.8 Hz), 6.93 (t, 1H, *J* = 7.6 Hz), 7.05 (d, 2H, *J* = 8.4 Hz), 7.10 (t, 1H, *J* = 6.8 Hz), 7.23 (d, 1H, *J* = 7.8 Hz), 7.28 (d, 2H, *J* = 8.4 Hz). ^{13}C NMR (75 MHz, $CDCl_3$): δ 26.2, 29.6, 34.9, 47.7, 123.9, 127.1, 127.4, 128.2, 129.8, 130.1 130.8, 135.1, 139.2, 143.7, 168.0. IR (ATR): λ (cm^{-1}) 2935, 2911, 1650, 1637, 1577, 1567, 1488, 1448, 1434, 1393, 1377, 1357, 1310, 1274, 1256, 1182, 1139, 1072, 1063, 1030, 1006, 954, 853, 841, 827, 760, 739, 625, 575, 550, 535. HRMS (ES) *m*/*z* calcd for $C_{17}H_{16}BrNO$ $[M + Na]^+$ 352.0307, found 352.0324. HPLC t_R = 21.1 min, purity 98.9% (254 nm).

*1-(4-Iodobenzoyl)-2,3,4,5-tetrahydro-1H-1-benzazepine (**11**).* Benzazepine **8** reacted with 4-iodobenzoic acid according to general method A to give **11** as a white solid (yield 38%). R_f = 0.4 (hept/AcOEt 7/3). MP = 137 °C. ^{1}H NMR (300 MHz, $CDCl_3$): δ 1.40−1.60 (m, 1H), 1.87−2.18 (m, 3H), 2.70−3.10 (m, 3H), 5.00 (d, 1H, *J* = 13.1 Hz), 6.62 (d, 1H, *J* = 7.5 Hz), 6.91 (d, 2H, *J* = 8.4 Hz), 6.93 (m, 1H), 7.10 (t, 1H, *J* = 7.5 Hz), 7.23 (d, 1H, *J* = 7.5 Hz), 7.48 (d, 2H, *J* = 8.4

DOI: 10.1021/acs.jmedchem.8b00697
J. Med. Chem. 2018, 61, 8670−8692

Hz). ^{13}C NMR (75 MHz, $CDCl_3$): δ 26.2, 29.5, 34.9, 47.7, 96.0, 127.1, 127.4, 128.2, 129.8, 130.1, 135.7, 136.8, 139.2, 143.7, 168.1. IR (ATR): λ (cm^{-1}) 2931, 2906, 2850, 2837, 1635, 1602, 1582, 1491, 1438, 1392, 1381, 1356, 1309, 1274, 1257, 1180, 1140, 1007, 950, 823, 765, 743, 660, 574, 552. HRMS (ES) m/z calcd for $C_{17}H_{16}INO$ $[M + H]^+$ 378.0349, found 378.0334. HPLC t_R = 21.7 min, purity 98.1% (254 nm).

*1-(4-Propylbenzoyl)-2,3,4,5-tetrahydro-1H-1-benzazepine (**12**).* Benzazepine **8** reacted with 4-*n*-propylbenzoic acid according to general method A to give **12** as a beige glass (yield 86%). R_f = 0.3 (hept/AcOEt 8/2). MP = 36 °C. ^{1}H NMR (300 MHz, $CDCl_3$): δ 0.85 (t, 3H, J = 7.4 Hz), 1.43−1.64 (m, 3H), 1.87−2.16 (m, 3H), 2.48 (t, 2H, J = 7.5 Hz), 2.76 (t, 1H, J = 11.6 Hz), 2.82−2.93 (m, 1H), 3.05 (t, 1H, J = 13.5 Hz), 5.04 (dl app, 1H, J = 14.1 Hz), 6.64 (d, 1H, J = 7.8 Hz), 6.84−6.92 (m, 1H), 6.94 (d, 2H, J = 8.1 Hz), 7.02−7.17 (m, 3H), 7.22 (d, 1H, J = 7.2 Hz). ^{13}C NMR (75 MHz, $CDCl_3$): δ 13.6, 24.1, 26.3, 29.7, 35.0, 37.7, 47.6, 126.8, 126.9, 127.7, 128.2, 128.3, 129.9, 133.5, 139.2, 144.3, 169.1. IR (ATR): λ (cm^{-1}) 2927, 2854, 1634, 1580, 1491, 1438, 1382, 1354, 1307, 1275, 1260, 1179, 1139, 955, 852, 808, 755, 740, 720, 578, 547, 485, 466, 438. HRMS (ES) m/z calcd for $C_{20}H_{23}NO$ $[M + H]^+$ 294.1852, found 294.1845. HPLC t_R = 20.3 min, purity 98.8% (254 nm).

*1-(4-Butylbenzoyl)-2,3,4,5-tetrahydro-1H-1-benzazepine (**13**).* Benzazepine **8** reacted with 4-*n*-butylbenzoic acid according to general method A to give **13** as a beige solid (yield 83%). R_f = 0.3 (hept/AcOEt 8/2). MP = 42 °C. ^{1}H NMR (300 MHz, $CDCl_3$): δ 0.87 (t, 3H, J = 7.1 Hz), 1.26 (sext, 2H, J = 7.3 Hz), 1.50 (quint, 2H, J = 7.4 Hz), 1.40−1.63 (m, 1H), 1.85−2.19 (m, 3H), 2.50 (t, 2H, J = 7.7 Hz), 2.66−2.95 (m, 2H), 3.05 (t, 1H, J = 13.3 Hz), 5.04 (d, 1H, J = 13.4 Hz), 6.64 (d, 1H, J = 7.6 Hz), 6.82−6.95 (m, 1H), 6.94 (d, 2H, J = 8.2 Hz), 7.00−7.12 (m, 1H), 7.10 (d, 2H, J = 7.8 Hz), 7.23 (dd, 1H, J = 7.4, 1.2 Hz). ^{13}C NMR (50 MHz, $CDCl_3$): δ 13.8, 22.2, 26.3, 29.7, 33.2, 35.0, 35.3, 47.6, 126.9, 126.9, 127.6, 128.2, 128.3, 129.9, 133.4, 139.2, 144.3, 144.5, 169.1. IR (ATR): λ (cm^{-1}) 2956, 2925, 2854, 1632, 1611, 1580, 1491, 1452, 1435, 1383, 1355, 1307, 1275, 1261, 1179, 1139, 954, 851, 837, 767, 748, 713, 579, 549. HRMS (ES) m/z calcd for $C_{21}H_{25}NO$ $[M + H]^+$ 308.2009, found 308.1994. HPLC t_R = 21.8 min, purity 98.9% (254 nm).

*1-(1,1′-Biphenyl-4-ylcarbonyl)-2,3,4,5-tetrahydro-1H-1-benzazepine (**14**).* Benzazepine **8** reacted with 4-phenylbenzoic acid according to general method A to give **14** as a white solid (yield 87%). R_f = 0.4 (hept/AcOEt 7/3). MP = 162 °C. ^{1}H NMR (300 MHz, $CDCl_3$): δ 1.36−1.63 (m, 1H), 1.77−2.20 (m, 3H), 2.60−3.20 (m, 3H), 5.06 (d, 1H, J = 13.9 Hz), 6.69 (d, 1H, J = 7.6 Hz), 6.92 (t, 1H, J = 7.1 Hz), 7.00−7.58 (m, 11H). ^{13}C NMR (75 MHz, $CDCl_3$): δ 26.3, 29.7, 35.0, 47.7, 126.2, 127.0, 127.1, 127.6, 128.3, 128.7, 130.0, 135.0, 139.2, 140.1, 142.1, 144.1, 168.8. IR (ATR): λ (cm^{-1}) 3061, 2939, 2924, 2914, 2881, 2852, 2837, 1626, 1615, 1575, 1557, 1488, 1454, 1441, 1434, 1402, 1385, 1355, 1310, 1274, 1258, 1139, 1110, 948, 854, 840, 775, 767, 756, 747, 735, 700, 676, 579. HRMS (ES) m/z calcd for $C_{23}H_{21}NO$ $[M + Na]^+$ 350.1515, found 350.1534. HPLC t_R = 22.6 min, purity 99.4% (254 nm).

*1-(4-Pyridin-3-ylbenzoyl)-2,3,4,5-tetrahydro-1H-1-benzazepine (**15**).* To a suspension of **5a** (232 mg, 0.987 mmol) in 6 mL of anhydrous THF under argon atmosphere were added $SOCl_2$ (0.36 mL, 4.935 mmol) and 3 drops of DMF. The mixture was stirred overnight at rt. The liquid was evaporated, and the residue was dissolved in 2 mL of anhydrous THF, evaporated again, and dried in vacuo. A solid was obtained. It was suspended with DMAP (3.0 mg, 0.024 mmol) in 6 mL of anhydrous CH_2Cl_2. A solution of **8** (120 mg, 0.815 mmol) and anhydrous pyridine (0.20 mL, 2.445 mmol) in 1 mL of anhydrous CH_2Cl_2 was added dropwise at 0 °C under argon atmosphere. Stirring was maintained 4 h at rt. The mixture was then diluted in 30 mL of CH_2Cl_2 and washed with 10 mL of 1 N HCl and 10 mL of a saturated aqueous $NaHCO_3$. The organic phase was dried over Na_2SO_4 and evaporated. The residue was purified by chromatography on a silica gel column (hept → hept/AcOEt 4/6). Recrystallization from EtOH afforded white crystals (130 mg; yield 49%). R_f = 0.3 (hept/AcOEt 25/75). MP = 128 °C. ^{1}H NMR (300 MHz, $CDCl_3$): δ 1.44−1.63 (m, 1H), 1.88−2.20 (m, 3H), 2.72−2.98 (m, 2H), 3.08 (t, 1H, J = 13.0 Hz), 5.05 (d, 1H, J = 13.2 Hz), 6.68 (d, 1H, J = 7.8 Hz), 6.93 (t, 1H, J = 7.4 Hz), 7.10 (t, 1H, J = 7.4 Hz), 7.20−7.40 (m, 2H), 7.30 (d, 2H, J = 8.1 Hz), 7.38 (d, 2H, J = 8.4 Hz), 7.79 (d, 1H, J = 7.8 Hz), 8.57 (d, 1H, J = 3.3 Hz), 8.76 (s, 1H). ^{13}C NMR (50 MHz, $CDCl_3$): δ 26.3, 29.6, 35.0, 47.7, 123.5, 126.3, 127.1, 127.3, 128.3, 129.0, 130.1, 134.2, 135.6, 136.0, 138.7, 139.3, 143.9, 148.2, 148.8, 168.4. IR (ATR): λ (cm^{-1}) 3052, 3033, 3004, 2930, 2855, 1632, 1576, 1495, 1435, 1393, 1358, 1315, 1278, 1259, 1143, 1003, 951, 854, 810, 761, 741, 715, 600, 583, 549, 409. HRMS (ES) m/z calcd for $C_{22}H_{20}N_2O$ $[M + H]^+$ 329.1648, found 329.1651. HPLC t_R = 14.4 min, purity 99.3% (254 nm).

*1-(4-Pyrimidin-2-ylbenzoyl)-2,3,4,5-tetrahydro-1H-1-benzazepine (**16**).* To a suspension of **5b** (164 mg, 0.821 mmol) in 8 mL of an anhydrous mixture of CH_2Cl_2/THF 1/1 under argon atmosphere were added $SOCl_2$ (0.18 mL, 2.463 mmol) and 3 drops of DMF. The mixture was stirred overnight at rt. Solvents were evaporated, and the residue was disolved in 2 mL of anhydrous THF, evaporated, and then dried in vacuo. The solid that was obtained was mixed with DMAP (2.5 mg, 0.020 mmol) in 5 mL of anhydrous CH_2Cl_2. A solution of benzazepine **8** (100 mg, 0.679 mmol) and anhydrous pyridine (0.16 mL, 2.040 mmol) in 1 mL of anhydrous CH_2Cl_2 was added dropwise to this suspension, at 0 °C under argon atmosphere. The mixture was stirred overnight at rt. It was then diluted with 20 mL of CH_2Cl_2 and washed with 10 mL of 1 N HCl and 10 mL of a saturated aqueous solution of $NaHCO_3$. The organic phase was then collected, dried on Na_2SO_4, and evaporated. The residue was purified on a chromatography on a silica gel column (hept → hept/AcOEt 6/4). Recrystallization from EtOH affords transparent crystals (158 mg; yield 70%). R_f = 0.6 (hept/AcOEt 25/75). MP = 173 °C. ^{1}H NMR (200 MHz, $CDCl_3$): δ 1.40−1.72 (m, 1H), 1.87−2.20 (m, 3H), 2.68−2.98 (m, 2H), 3.09 (t, 1H, J = 12.9 Hz), 5.05 (d app, 1H, J = 13.4 Hz), 6.66 (d, 1H, J = 7.6 Hz), 6.87 (t, 1H, J = 7.5 Hz), 7.05 (t, 1H, J = 7.4 Hz), 7.11−7.36 (m, 2H), 7.31 (d, 2H, J = 8.2 Hz), 8.23 (d, 2H, J = 8.4 Hz), 8.76 (d, 2H, J = 4.6 Hz). ^{13}C NMR (50 MHz, $CDCl_3$): δ 26.4 29.6, 35.0, 47.7, 119.3, 127.0, 127.3, 127.4, 128.3, 130.0, 138.3, 138.4, 139.3, 143.8, 157.2, 164.0, 168.8. IR (ATR): λ (cm^{-1}) 3066, 3050, 2922, 2882, 2853, 1628, 1575, 1566, 1556, 1494, 1417, 1404, 1385, 1356, 1313, 1279, 1260, 1142, 1018, 953, 866, 815, 804, 778, 761, 752, 744, 656, 641, 627, 582, 550, 476. HRMS (ES) m/z calcd for $C_{21}H_{19}N_3O$ $[M + H]^+$ 330.1601, found 330.1596. HPLC t_R = 20.2 min, purity 99.9% (254 nm).

*1-[4-(3-Methyl-1H-pyrazol-1-yl)benzoyl]-2,3,4,5-tetrahydro-1H-1-benzazepine (**17**).* Benzazepine **8** reacted with the acid **3a** according to general method A to give **17** as transparent crystals after recrystallization from AcOEt (yield 88%). R_f = 0.4 (hept/AcOEt 5/5). MP = 124 °C. ^{1}H NMR (200 MHz, $CDCl_3$): δ 1.40−1.65 (m, 1H), 1.80−2.20 (m, 3H), 2.32 (s, 3H), 2.65−3.20 (m, 3H), 5.03 (d, 1H, J = 13.2 Hz), 6.20 (d, 1H, J = 2.2 Hz), 6.64 (d, 1H, J = 7.8 Hz), 6.89 (t, 1H, J = 7.6 Hz), 7.06 (td, 1H, J = 7.6, 1.0 Hz), 7.15−7.35 (m, 3H), 7.43 (d, 2H, J = 8.6 Hz), 7.74 (d, 1H, J = 2.4 Hz). ^{13}C NMR (75 MHz, $CDCl_3$): δ 13.6, 26.2, 29.5, 34.9, 47.6, 107.9, 117.3, 127.0, 127.2, 127.2, 128.2, 129.5, 129.9, 133.4, 139.1, 140.4, 143.9, 150.9, 168.1. IR (KBr): λ (cm^{-1}) 3054, 2933, 2854, 1638, 1611, 1579, 1542, 1491, 1452, 1439, 1426, 1398, 1384, 1360, 1309, 1275, 1258, 1226, 1177, 1140, 1047, 958, 945, 837, 772, 758, 577. HRMS (ES) m/z calcd for $C_{21}H_{21}N_3O$ $[M + H]^+$ 332.1757, found 332.1746. HPLC t_R = 18.9 min, purity 99.2% (254 nm). Elemental analysis calculated (%) for $C_{21}H_{21}N_3O$: C 76.11, H 6.39, N 12.68. Found: C 75.92, H 6.66, N 12.68.

*1-(4-Nitrobenzoyl)-2,3,4,5-tetrahydro-1H-1-benzazepine (**18**).* A mixture of benzazepine **8** (258 mg, 1.75 mmol) and anhydrous pyridine (0.70 mL, 8.76 mmol) in 3 mL of anhydrous CH_2Cl_2 was added dropwise to a solution of 4-nitrobenzoyl chloride (390 mg, 2.10 mmol) in 10 mL of anhydrous CH_2Cl_2 under argon atmosphere at 0 °C. The mixture was stirred for 45 min at 0 °C and one night at rt. The products were poured into 10 mL of water and extracted twice with 30 mL of CH_2Cl_2. The organic phase was washed with 20 mL of 0.5 N HCl and 20 mL of water, dried over Na_2SO_4, and evaporated. The residue was purified by chromatography on a silica gel column (hept/AcOEt 7/3 → 6/4) affording white crystals (360 mg; yield 69%). R_f = 0.3 (hept/AcOEt 7/3). MP = 141 °C. ^{1}H NMR (200 MHz, $CDCl_3$): δ 1.40−1.70 (m, 1H), 1.85−2.25 (m, 3H), 2.70−3.15 (m, 3H), 4.99 (d, 1H, J = 13.4 Hz), 6.60 (d, 1H, J = 7.6 Hz), 6.91 (td, 1H, J = 7.7, 1.7 Hz), 7.11 (td,

DOI: 10.1021/acs.jmedchem.8b00697
J. Med. Chem. 2018, 61, 8670−8692

1H, J = 7.5, 1.2 Hz), 7.25 (d, 1H), 7.35 (d, 2H, J = 9.0 Hz), 8.01 (d, 2H, J = 9.0 Hz). ^{13}C NMR (75 MHz, $CDCl_3$): δ 26.3, 29.5, 35.0, 47.8, 123.0, 127.2, 127.9, 128.2, 128.8, 130.4, 139.4, 142.5, 142.9, 147.9, 168.4. IR (KBr): λ (cm^{-1}) 3102, 3074, 2939, 2916, 2849, 1642, 1598, 1513, 1491, 1440, 1412, 1344, 1316, 1271, 861, 765, 735.

*1-(4-Aminobenzoyl)-2,3,4,5-tetrahydro-1H-1-benzazepine (**19**).* A few mg of 10% Pd/C were added to compound **18** (356 mg, 1.20 mmol) in 10 mL of EtOH and 10 mL of AcOEt and the suspension was stirred under H_2 (20 psi) at rt for 5 h. The mixture was then filtered on Celite, and the filtrate was evaporated. The residue was taken up in 50 mL of CH_2Cl_2 and washed with 40 mL of water. The organic phase was dried over Na_2SO_4 and evaporated. Compound **19** was obtained as a white powder (326 mg; quantitative yield). R_f = 0.3 (hept/AcOEt 5/5). MP = 162 °C. ^{1}H NMR (300 MHz, $CDCl_3$): δ 1.49 (m, 1H), 1.70−2.20 (m, 3H), 2.50−3.10 (m, 3H), 3.15−4.00 (bs, 1H), 5.02 (m, 1H), 6.38 (d, 2H, J = 8.1 Hz), 6.67 (d, 1H, J = 7.8 Hz), 6.93 (t, 1H, J = 7.6 Hz), 7.02 (d, 2H, J = 8.1 Hz), 7.07 (t, 1H, J = 7.5 Hz), 7.22 (d, 1H, J = 7.5 Hz). ^{13}C NMR (75 MHz, $CDCl_3$): δ 26.2, 29.7, 34.9, 47.6, 113.7, 125.8, 126.7, 126.9, 128.2, 129.9, 130.4, 139.0, 144.8, 147.5, 168.9. IR (KBr): λ (cm^{-1}) 3447, 3351, 2931, 2838, 1617, 1383, 1308, 1273, 1170, 764, 503. HRMS (ES) m/z calcd for $C_{18}H_{20}NO$ $[M + H]^+$ 267.1492, found 267.1477. HPLC t_R = 17.8 min, purity 99.2% (254 nm). Elemental analysis calculated (%) for $C_{18}H_{20}NO$: C 76.66, H 6.81, N 10.52. Found: C 76.50, H 6.98, N 10.29.

*N,N,N-Trimethyl-4-(2,3,4,5-tetrahydro-1H-1-benzazepin-1-ylcarbonyl)benzenaminium (**20**).* A solution of **19** (400 mg, 1.50 mmol), MeI (0.20 mL, 3.00 mmol), and K_2CO_3 (311 mg, 2.25 mmol) in 8 mL of CH_2Cl_2 was warmed at 70 °C under argon atmosphere during 6 h. After return to rt, the mixture was poured into 50 mL of water and extracted with 80 mL of AcOEt/toluene. The organic phase was washed with 25 mL of water, dried over Na_2SO_4, and evaporated. Recrystallization from MeOH afforded white crystals (293 mg, yield 66%). R_f = 0.6 (hept/AcOEt 5/5). MP = 152 °C. ^{1}H NMR (300 MHz, $CDCl_3$): δ 1.45 (m, 1H), 1.75−2.20 (m, 3H), 2.50−3.20 (m, 9H), 4.90−5.30 (m, 1H), 6.34 (d, 2H, J = 7.9 Hz), 6.66 (m, 1H), 6.89 (m, 1H), 7.00−7.40 (m, 4H). ^{13}C NMR (75 MHz, $CDCl_3$): δ 25.9, 29.5, 34.6, 39.6, 47.3, 110.0, 122.3, 126.3, 126.6, 127.8, 129.6, 130.1, 138.6, 144.8, 150.7, 168.6. IR (KBr): λ (cm^{-1}) 3094, 3007, 2933, 2845, 1612, 1524, 1484, 1437, 1369, 1302, 1194, 1169, 762, 500. HRMS (ES) m/z calcd for $C_{19}H_{22}N_2O$ $[M + H]^+$ 295.1805, found 295.1798. HPLC t_R = 21.1 min, purity 98.8% (254 nm). Elemental analysis calculated (%) for $C_{19}H_{22}N_2O$: C 77.52, H 7.53, N 9.52. Found: C 77.69, H 7.75, N 9.62.

*N,N,N-Trimethyl-4-(2,3,4,5-tetrahydro-1H-1-benzazepin-1-ylcarbonyl)benzenaminium, Trifluoroacetate (**21**).* To a solution of **20** (80 mg, 0.273 mmol) in 10 mL of anhydrous CH_2Cl_2 under argon atmosphere were added $AgClO_4$ (62 mg, 0.300 mmol) then MeI (19 μL, 0.300 mmol). The mixture was stirred for 2 h at rt in the dark, then filtered, and the solvent was evaporated. The residue was purified by semipreparative HPLC (H_2O/0.1% TFA) for 5 min, then from 0 to 100% of MeCN/0.1% TFA in H_2O/0.1% TFA from 5 to 30 min, at a flow rate of 10 mL/min. After lyophilization, compound **21** was obtained as a hygroscopic white powder (49 mg; yield 42%). R_f = 0.2 (CH_2Cl_2/MeOH 8/2). MP = 60 °C. ^{1}H NMR (300 MHz, $CDCl_3$): δ 1.53 (m, 1H), 1.90−2.20 (m, 3H), 2.35 (bs, 2H), 2.72−2.92 (m, 2H), 3.03 (t, 1H, J = 12.9 Hz), 3.75 (s, 9H), 4.95 (d, 1H, J = 12.9 Hz), 6.60 (d, 1H, J = 7.5 Hz), 6.92 (t, 1H, J = 7.6 Hz), 7.11 (t, 1H, J = 7.4 Hz, H_9), 7.24 (d, 1H, J = 7.2 Hz, H_8), 7.37 (d, 2H, J = 8.7 Hz, $H_{15a,b}$), 7.70 (d, 2H, J = 9.0 Hz). ^{13}C NMR (75 MHz, $CDCl_3$): δ 26.2, 29.5, 34.8, 47.9, 57.0, 119.4, 127.2, 128.0, 128.1, 130.2, 130.4, 138.8, 139.3, 142.8, 147.3, 160.9, 161.2, 166.5. IR (ATR): λ (cm^{-1}) 3417, 3042, 2930, 2854, 1683, 1633, 1579, 1492, 1455, 1442, 1414, 1396, 1358, 1314, 1277, 1198, 1168, 1146, 1118, 1071, 1016, 956, 940, 847, 824, 800, 761, 749, 717, 598. HRMS (ES) m/z calcd for $C_{20}H_{25}N_2O{\cdot}C_2F_3O_2{\cdot}H_2O$ $[M]^+$ 309.1961, found 309.1961. Elemental analysis calculated (%) for $C_{20}H_{25}N_2O{\cdot}C_2F_3O_2{\cdot}H_2O$: C 59.99, H 6.18, N 6.36. Found: C 59.21, H 6.56, N 6.18.

*N-[4-(2,3,4,5-Tetrahydro-1H-1-benzazepin-1-ylcarbonyl)phenyl]-acetamide (**22**).* A solution of **19** (60 mg, 0.225 mmol), Ac_2O (25 μL, 0.248 mmol), and DIEA (60 μL, 0.338 mmol) in 1.5 mL of anhydrous CH_2Cl_2 was stirred for 4 h at rt. The mixture was then diluted with 10 mL of CH_2Cl_2, and the organic phase was washed with 5 mL of water, 5 mL of 10% citric acid, and 5 mL of saturated aqueous Na_2CO_3. The aqueous phases were extracted again with 40 mL of CH_2Cl_2. The organic phases were gathered, dried over Na_2SO_4, and evaporated. The residue was purified by chromatography on silica gel column (hept/AcOEt 5/5 → 1/9). Compound **22** was obtained as a white powder (68 mg; yield 98%). R_f = 0.5 (hept/AcOEt 1/9). MP = 168 °C. ^{1}H NMR (300 MHz, $CDCl_3$): δ 1.51 (m, 1H, 1.75−2.00 (m, 3H), 2.09 (s, 3H), 2.65−3.10 (m, 3H), 5.00 (d, 1H, J = 13.5 Hz), 6.61 (d, 1H, J = 7.5 Hz), 6.89 (t, 1H, J = 7.2 Hz), 7.00−7.15 (m, 3H), 7.21 (d, 1H, J = 7.2 Hz), 7.20−7.40 (m, 2H), 7.72 (bs, 1H). ^{13}C NMR (50 MHz, $CDCl_3$): δ 24.6, 26.2, 29.6, 34.9, 47.7, 118.3, 127.0, 127.2, 128.2, 129.2, 130.0, 131.4, 139.1, 139.3, 144.0, 168.5, 168.6. IR (KBr): λ (cm^{-1}) 3289, 3036, 2925, 2861, 1691, 1620, 1529, 1406, 1308, 1262, 503. HRMS (ES) m/z calcd for $C_{19}H_{20}N_2O_2$ $[M + H]^+$ 309.1598, found 309.1587. HPLC t_R = 14.2 min, purity 99.0% (254 nm). Elemental analysis calculated (%) for $C_{19}H_{20}N_2O_2$: C 74.00, H 6.54, N 9.08. Found: C 74.04, H 6.75, N 9.15.

*1-[4-[(1,1′-Biphenyl-2-ylcarbonyl)amino]benzoyl]-2,3,4,5-tetrahydro-1H-1-benzazepine (**23**).* To a solution of 2-biphenylcarboxylic acid (113 mg, 0.56 mmol) in 1.5 mL of anhydrous CH_2Cl_2 at 0 °C under argon atmosphere were added 3−4 drops of DMF and $(COCl)_2$ (70 μL, 0.76 mmol). The mixture was stirred for 2 h at 0 °C. The CH_2Cl_2 was evaported and the residue dissolved in 1.5 mL of anhydrous CH_2Cl_2. This solution was added dropwise, at 0 °C under argon to a mixture of **19** (30 mg, 0.11 mmol) and NEt_3 (80 μL, 0.56 mmol) in 1.5 mL of anhydrous CH_2Cl_2. The mixture was stirred 2 h between 0 and 10 °C before being washed with 3 mL of H_2O, 3 mL of 10% acetic acid, and 3 mL of saturated aqueous $NaHCO_3$. The organic phase was dried over Na_2SO_4 and evaporated. The residue was purified by chromatography on a silica gel column (CH_2Cl_2→ CH_2Cl_2/MeOH 98/2). Compound **23** was obtained as a white powder (37 mg; yield 75%). R_f = 0.6 (CH_2Cl_2/MeOH 9/1). MP = 201 °C. ^{1}H NMR (300 MHz, $CDCl_3$): δ 1.40−1.60 (m, 1H), 1.80−2.20 (m, 3H), 2.60−3.20 (m, 3H), 4.99 (d, 1H, J = 12.8 Hz), 6.60 (d, 1H, J = 7.5 Hz), 6.80−7.20 (m, 7H), 7.21 (d, 1H, J = 7.5 Hz), 7.30−7.70 (m, 8H), 7.82 (d, 1H, J = 7.5 Hz). ^{13}C NMR (75 MHz, $CDCl_3$): δ 26.6, 30.0, 35.3, 48.1, 118.6, 127.5, 128.3, 128.5, 128.6, 129.1, 129.3, 129.6, 123.0, 130.4, 130.7, 131.2, 132.2, 135.3, 139.1, 139.5, 140.1, 144.5, 167.4, 168.7. IR (KBr): λ (cm^{-1}) 3250, 3178, 3094, 3036, 2945, 2931, 1691, 1607, 1529, 1445, 1406, 1315, 1250, 743, 503. HRMS (ES) m/z calcd for $C_{30}H_{26}N_2O_2$ $[M + H]^+$ 447.2067, found 447.2043. HPLC t_R = 21.5 min, purity 98.2% (254 nm). Elemental analysis calculated (%) for $C_{30}H_{26}N_2O_2$: C 80.69, H 5.87, N 6.27. Found: C 79.98, H 6.12, N 6.20.

*1-[2-Chloro-4-(3-methyl-1H-pyrazol-1-yl)benzoyl]-2,3,4,5-tetrahydro-1H-1-benzazepine (**38**).* Compound **38** was prepared according to general method A, affording a creamy powder (yield 61%). R_f = 0.4 (hept/AcOEt 5/5). MP = 112−114 °C (lit:[61] 117−120 °C). ^{1}H NMR (200 MHz, $CDCl_3$): δ 1.40−1.80 (m, 1H), 1.85−2.20 (m, 3H), 2.32 (s, 2.59H), 2.39 (s, 0.41H), 2.70−2.95 (m, 2H), 3.05 (t, 1H, J = 13.0 Hz), 4.95 (d, 1H, J = 13.4 Hz), 6.21 (d, 0.87H, J = 2.4 Hz), 6.30 (d, 0.13H, J = 2.4 Hz), 6.83−7.17 (m, 5.10H), 7.31 (d, 0.56H, J = 2.0 Hz), 7.38−7.58 (m, 0.43H), 7.62 (d, 0.81H, J = 2.0 Hz), 7.70 (d, 0.93H, J = 2.4 Hz), 7.84 (t, 0.18H, J = 2.1 Hz). ^{13}C NMR (50 MHz, $CDCl_3$): δ 13.6, 26.4, 29.3, 35.0, 47.5, 108.3, 115.8, 119.3, 127.0, 127.3, 127.4, 127.6, 128.4, 130.0, 132.2, 133.9, 139.4, 140.5, 142.4, 151.3, 166.3. IR (KBr): λ (cm^{-1}) 3147, 3024, 2929, 2853, 1650, 1602, 1396, 1314, 759. HRMS (ES) m/z calcd for $C_{21}H_{20}ClN_3O$ $[M + H]^+$ 366.1368, found 366.1360. HPLC t_R = 20.5 min, purity 98.5% (254 nm). Elemental analysis (%) calculated for $C_{21}H_{20}ClN_3O$: C 68.94, H 5.51, N 11.49. Found: C 68.93, H 5.96, N 10.83.

*1-[4-(3-Methyl-1H-pyrazol-1-yl)benzoyl]-1,2,3,4-tetrahydro-5H-1-benzazepin-5-one (**39a**).* Compound **39a** was prepared from the amine **26** and the acid **3a** according to general method A, affording yellow crystals after recrystallization from EtOH (yield 32%). R_f = 0.4 (hept/AcOEt 5/5). MP = 140 °C. ^{1}H NMR (300 MHz, $CDCl_3$): δ 2.18 (m, 2H), 2.34 (s, 3H), 2.92 (t, 2H, J = 6.2 Hz), 6.24 (d, 1H, J = 2.2 Hz), 6.74 (d, 1H, J = 7.8 Hz), 7.23 (m, 2H), 7.31 (d, 2H, J = 8.7 Hz), 7.49 (d, 2H, J = 8.7 Hz), 7.76 (d, 1H, J = 2.2 Hz), 7.87 (dd, 1H, J = 7.8, 1.6 Hz). ^{13}C NMR (50 MHz, $CDCl_3$): δ 14.1, 23.0, 40.6, 47.9, 108.7, 118.0,

DOI: 10.1021/acs.jmedchem.8b00697
J. Med. Chem. 2018, 61, 8670−8692

127.7, 127.8, 129.4, 129.9, 130.6, 132.8, 133.5, 134.5, 141.5, 143.2, 151.7, 169.8, 202.4. IR (KBr): λ (cm^{-1}) 3600−3200, 3130, 3061, 2929, 2901, 2873, 1680, 1639, 1604, 1535, 1354, 1264, 772. HRMS (ES) m/z calcd for $C_{21}H_{19}N_3O_2$ $[M + H]^+$ 346.1550, found 346.1537. HPLC t_R = 23.1 min, purity 99.1% (254 nm). Elemental analysis (%) calculated for $C_{21}H_{19}N_3O_2$: C 73.03, H 5.54, N 12.17. Found: C 72.67, H 5.61, N 12.01.

*1-[2-Chloro-4-(3-methyl-1H-pyrazol-1-yl)benzoyl]-1,2,3,4-tetrahydro-5H-1-benzazepin-5-one (**39b**).* Compound **39b** was prepared from the amine **26** and the acid **3b** according to general method A, affording a beige powder (yield 30%). R_f = 0.3 (hept/AcOEt 5/5). MP = 147 °C. ^{1}H (200 MHz, $CDCl_3$): δ 2.14 (m, 2H), 2.33 (s, 3H), 2.90 (t, 2H, J = 6.0 Hz), 6.23 (d, 1H, J = 2.2 Hz), 6.96 (dd, 1H, J = 5.6, 3.4 Hz), 7.02−7.17 (m, 1H), 7.20−7.30 (m, 2H), 7.35 (d, 1H, J = 8.1 Hz), 7.58 (s, 1H), 7.71 (d, 1H, J = 2.4 Hz), 7.76 (dd, 1H, J = 5.9, 3.4 Hz). ^{13}C NMR (50 MHz, $CDCl_3$): δ 14.0, 22.2, 40.4, 46.6, 109.0, 116.3, 119.7, 127.7, 128.6, 128.8, 129.9, 133.4, 133.5, 135.7, 140.4, 141.3, 152.0, 168.3, 202.7. IR (KBr): λ (cm^{-1}) 3600−3200, 3123, 3068, 3040, 2929, 2874, 1681, 1639, 1604, 1382, 758. HRMS (ES) m/z calcd for $C_{21}H_{18}ClN_3O_2$ $[M + H]^+$ 380.1160, found 380.1161. HPLC t_R = 23.5 min, purity 95.8% (254 nm). Elemental analysis (%) calculated for $C_{21}H_{18}ClN_3O_2$: C 66.40, H 4.78, N 11.06. Found: C 67.41, H 5.51, N 10.22.

*1-[4-(3-Methyl-1H-pyrazol-1-yl)benzoyl]-2,3,4,5-tetrahydro-1H-1-benzazepin-5-ol (**40a**).* Compound **39a** (1.0 eq, 0.015M) and $NaBH_4$ (1.5 equiv) were stirred in MeOH for 2 h at rt. After evaporation of the solvent, the residue was dissolved in AcOEt and washed with H_2O. The organic phase was dried on Na_2SO_4 and evaporated to dryness. Column chromatography (gradient hept/AcOEt) afforded a beige powder (yield 95%). R_f = 0.4 (hept/AcOEt 2/8). MP = 178 °C. ^{1}H NMR (200 MHz, $CDCl_3$): δ 1.60−2.30 (m, 4H), 2.34 (s, 3H), 2.83 (t, J = 12.0 Hz, 1H), 4.70−5.30 (m, 2H,), 6.21 (d, 1H, J = 2.2 Hz), 6.63 (d, 1H, J = 7.6 Hz), 6.96 (t app, 1H, J = 7.3 Hz), 7.15−7.35 (m, 2H), 7.43 (d, 2H, J = 8.3 Hz), 7.54 (m, 1H), 7.66 (d, 1H, J = 7.6 Hz), 7.74 (d, 1H, J = 2.0 Hz). ^{13}C NMR (50 MHz, $CDCl_3$): δ 13.6, 23.1, 25.9, 29.7, 32.9, 35.7, 46.8, 48.0, 71.0, 74.9, 108.0, 117.5, 124.7, 127.3, 127.5, 128.1, 129.7, 130.3, 132.9, 140.2, 140.7, 141.1, 151.1, 168.3. IR (KBr): λ (cm^{-1}) 3434, 3372, 3268, 3117, 2925, 2856, 1631, 1604, 1535, 1432, 1383, 1356, 1307, 1260, 1053, 757, 503. HRMS (ES) m/z calcd for $C_{21}H_{21}N_3O_2$ $[M + H]^+$ 348.1707, found 348.1691. HPLC t_R = 20.9 min, purity 99.9% (254 nm). Elemental analysis (%) calculated for $C_{21}H_{21}N_3O_2$: C 72.60, H 6.09, N 12.09. Found: C 72.14, H 6.01, N 11.70.

*1-[2-Chloro-4-(3-methyl-1H-pyrazol-1-yl)benzoyl]-2,3,4,5-tetrahydro-1H-1-benzazepin-5-ol (**40b**).* Compound **39b** (1.0 eq, 0.015M) and $NaBH_4$ (1.5 equiv) were stirred in MeOH for 2 h at rt. After evaporation of the solvent, the residue was dissolved in AcOEt and washed with H_2O. The organic phase was dried on Na_2SO_4 and evaporated to dryness. Column chromatography (gradient hept/AcOEt) afforded a beige powder (yield 73%). R_f = 0.4 (hept/AcOEt 2/8). MP = 68 °C. ^{1}H NMR (300 MHz, $CDCl_3$): δ 1.60−2.30 (m, 4 H), 2.33 (s, 2 H), 2.39 (s, 1 H), 2.88 (t, 1 H, J = 12.2 Hz), 4.70−5.20 (m, 2 H), 6.22 (d, 0.78 H, J = 2.5 Hz), 6.31 (d, 0.22 H, J = 2.5 Hz), 6.85−7.10 (m, 3 H), 7.18 (t, 1 H, J = 7.6 Hz), 7.25−7.50 (m, 1 H), 7.57 (d, 0.72 H, J = 7.8 Hz), 7.62 (d, 0.86 H, J = 1.9 Hz), 7.70 (d, 1 H, J = 2.2 Hz), 7.84 (m, 1 H). ^{13}C NMR (75 MHz, $CDCl_3$): δ 13.6, 22.6, 25.7, 33.1, 35.9, 46.5, 47.7, 71.1, 74.9, 108.2, 108.4, 115.7, 115.8, 116.9, 119.2, 119.3, 124.4, 127.3, 127.5, 127.8, 128.4, 128.8, 129.8, 130.1, 132.2, 133.5, 138.3, 138.7, 140.6, 141.2, 142.0, 151.2, 151.4,166.5. IR (KBr): λ (cm^{-1}) 3392, 3124, 2925, 2856, 1638, 1604, 1535, 1445, 1411, 1362, 1315, 1053, 757. HRMS (ES) m/z calcd for $C_{21}H_{20}ClN_3O_2$ $[M + H]^+$ 382.1317, found 382.1316. HPLC t_R = 23.2 min, purity 99.6% (254 nm). Elemental analysis (%) calculated for $C_{21}H_{20}ClN_3O_2 \cdot H_2O$: C 63.08, H 5.55, N 10.51. Found: C 63.69, H 5.34, N 10.31.

*N,N-Dimethyl-1-[4-(3-methyl-1H-pyrazol-1-yl)benzoyl]-2,3,4,5-tetrahydro-1H-1-benzazepin-5-amine (**41a**).* Compound **41a** was prepared from the amine **28** and the acid **3a** according to general method A, affording white crystals after recrystallization from MeOH (yield 70%). R_f = 0.5 (AcOEt/MeOH 9/1). MP = 156 °C. ^{1}H NMR (200 MHz, $CDCl_3$): δ 1.10−2.00 (m, 4H, 2.19 (s, 3H), 2.34 (s, 3H), 2.45 (s, 3H), 2.60−5.20 (m, 3H), 6.22 (d, 1H, J = 1.9 Hz), 6.60 (d, 1H, J = 8.1 Hz), 6.95 (t, 1H), 7.10−7.35 (m, 3H), 7.46 (d, 2H, J = 8.3 Hz), 7.60 (d, 1H, J = 8.1 Hz), 7.76 (d, 1H, J = 2.0 Hz). ^{13}C NMR (50 MHz, $CDCl_3$): δ 13.7, 23.1, 24.3, 28.8, 29.6, 43.9, 44.9, 46.5, 48.0, 65.4, 107.8, 108.0, 117.4, 126.3, 127.3, 127.6, 128.7, 129.9, 131.4, 132.4, 133.1, 140.7, 151.0, 168.9. IR (KBr): λ (cm^{-1}) 3097, 2952, 2923, 2882, 2824, 2788, 1638, 1608, 1539, 1481, 1451, 1353, 759, 504. HRMS (ES) m/z calcd for $C_{23}H_{26}N_4O$ $[M + H]^+$ 375.2179, found 375.2166. HPLC mixture of diastereoisomers: t_R = 15.6 min (46.3%), t_R = 15.9 min (52.7%), purity 99.0% (254 nm). Elemental analysis (%) calculated for $C_{23}H_{26}N_4O$: C 73.77, H 7.00, N 14.96. Found: C 73.17, H 6.97, N 14.91.

*1-[2-Chloro-4-(3-methyl-1H-pyrazol-1-yl)benzoyl]-N,N-dimethyl-2,3,4,5-tetrahydro-1H-1-benzazepin-5-amine (**41b**).* Compound **41b** was prepared from the amine **28** and the acid **3b** according to general method A, affording white crystals after recrystallization from MeOH (yield 17%). R_f = 0.5 (AcOEt/MeOH 9/1). MP = 182 °C. ^{1}H NMR (200 MHz, $CDCl_3$): δ 1.10−2.00 (m, 4H), 2.19 (s, 3H), 2.33 (s, 3H), 2.39 (s, 3H), 2.60−5.20 (m, 3H), 6.23 (s, 0.77 H), 6.30 (d, 0.23H, J = 2.4 Hz), 6.80−7.17 (m, 3H), 7.17−7.45 (m, 2.74H), 7.17−7.68 (m, 1.81 Hz), 7.72 (d, 0.88H, J = 2.2 Hz), 7.79 (bs, 0.33H), 7.84 (d, 0.24H, J = 2.4 Hz). ^{13}C NMR (50 MHz, $CDCl_3$): δ 13.6, 23.0, 24.1, 29.0, 29.9, 43.9, 44.7, 45.3, 46.1, 47.6, 64.9, 72.5, 108.2, 108.4, 115.7, 115.8, 116.9, 119.0, 119.2, 126.2, 126.8, 127.1, 127.3, 127.8, 127.9, 128.2, 128.7, 129.1, 129.9, 132.3, 134.5, 137.9, 138.4, 140.3, 140.6, 140.9, 142.3, 151.2, 151.4, 166.4, 167.0. IR (KBr): λ (cm^{-1}) 3087, 2980, 2944, 2867, 2820, 2773, 1645, 1604, 1450, 1360, 1050, 759, 504. HRMS (ES) m/z calcd for $C_{23}H_{25}ClN_4O$ $[M + H]^+$ 409.1790, found 409.1785. HPLC, mixture of diastereoisomers: t_R = 16.1 min (30.7%), t_R = 16.5 min (67.0%); purity 97.7% (254 nm). Elemental analysis (%) calculated for $C_{23}H_{25}ClN_4O$: C 67.56, H 6.16, N 13.70. Found: C 67.54, H 6.28, N 13.63.

*10-[2-Chloro-4-(3-methyl-1H-pyrazol-1-yl)benzoyl]-10,11-dihydro-5H-pyrrolo[2,1-c][1,4]benzodiazepine (**42**; WAY-VNA-932).*[54] Compound **42** was prepared from the amine **31** and the acid **3b** according to general method A, affording a white powder (yield 43%). R_f = 0.4 (hept/AcOEt 5/5). MP = 105−108 °C. ^{1}H NMR (300 MHz, $CDCl_3$): δ 2.33 (s, 2.31H), 2.37 (s, 0.69H), 4.60−5.40 (m, 4H), 6.07 (m, 2H), 6.23 (d, 0.79H, J = 2.2 Hz), 6.30 (m, 0.21H), 6.68 (bs, 1H), 6.95−7.56 (m, 6H), 7.61 (d, 0.80H, J = 1.7 Hz), 7.72 (d, 0.80H, J = 2.2 Hz), 7.84 (m, 0.40H). ^{13}C NMR (75 MHz, $CDCl_3$): δ 13.7, 45.7, 51.1, 107.6, 108.6, 109.0, 115.9, 119.3, 121.7, 125.7, 127.3, 127.9, 128.5, 128.6, 129.1, 129.8, 132.3, 133.1, 134.6, 140.3, 140.8, 151.5, 167.3. IR (KBr): λ (cm^{-1}) 3122, 2953, 2953, 2861, 1648, 1606, 1529, 1500, 1366, 1049, 759, 710, 505. HRMS (ES) m/z calcd for $C_{23}H_{19}ClN_4O$ $[M + H]^+$ 403.1320, found 403.1316. HPLC t_R = 21.2 min, purity 97.5% (254 nm). Elemental analysis (%) calculated for $C_{23}H_{19}ClN_4O$: C 68.57, H 4.75, N 13.91. Found: C 68.58, H 5.26, N 13.04.

*5-[2-Chloro-4-(3-methyl-1H-pyrazol-1-yl)benzoyl]-1-methyl-1,4,5,10-tetrahydro pyrazolo[3,4-b][1,5]benzodiazepine (**43**).* Compound **43** was prepared from the amine **37** (182 mg, 0.907 mmol) and the acid **3b** (280 mg, 1.18 mmol) according to general method A, as was previously described.[49]

*1-[2-Chloro-4-(3-methyl-1H-pyrazol-1-yl)benzoyl]azepane (**44**).* Compound **44** was prepared from the azepine and the acid **3b** according to general method A, affording a white powder (22 mg; yield 35%). R_f = 0.3 (hept/AcOEt 5/5). MP = 100 °C. ^{1}H NMR (300 MHz, $CDCl_3$): δ 1.40−2.00 (m, 8H), 2.35 (s, 3H), 3.20−3.40 (m, 2H), 3.55−3.90 (dt, 2H, J = 18.6, 5.6 Hz), 6.25 (d, 1H, J = 2.2 Hz), 7.30 (d, 1H, J = 8.3 Hz), 7.56 (dd, 1H, J = 8.3, 1.9 Hz), 7.74 (d, 1H, J = 1.9 Hz), 7.79 (d, 1H, J = 2.2 Hz). ^{13}C NMR (75 MHz, $CDCl_3$): δ 13.7, 26.5, 27.3, 27.7, 28.9, 45.6, 49.0, 108.7, 116.8, 119.6, 127.4, 128.4, 131.3, 134.0, 140.8, 151.4, 167.7. IR (KBr): λ (cm^{-1}) 3118, 2926, 2856, 1622, 1603, 1539, 1482, 1437, 1378, 1359, 1306, 1057, 882, 757. HRMS (ES) m/z calcd for $C_{17}H_{20}ClN_3O$ $[M + H]^+$ 318.1368, found 318.1356. HPLC t_R = 24.9 min, purity 99.2% (254 nm).

*(S)-tert-Butyl 2-(Dimethylcarbamoyl)pyrrolidine-1-carbamate (**46**).* A solution of (*S*) Boc-proline (1 equiv), trimethylamine (2 equiv), and HOBt (1.2 equiv) in CH_2Cl_2 was stirred for 20 min at rt. Dimethylamine hydrochloride (1 equiv) was then added. The mixture

DOI: 10.1021/acs.jmedchem.8b00697
J. Med. Chem. 2018, 61, 8670−8692

was stirred for 20 h at rt. CH_2Cl_2 was then added, and the mixture was washed with 0.3 M aqueous potassium sulfate, saturated aqueous sodium bicarbonate, and brine. The organic phase was dried over Na_2SO_4 and evaporated in vacuo. The expected compound was obtained after purification by chromatography on silica gel column (AcOEt, 1% Et_3N) to afford a colorless oil (yield 75%). R_f = 0.55 (Hept/AcOEt, 1/1). ^{1}H NMR (400 MHz, $CDCl_3$): δ 4.68−4.47 (m, 1H), 3.63−3.34 (m, 2H), 3.14−2.86 (m, 6H), 2.19−1.94 (m, 2H), 1.89−1.74 (m, 2H), 1.44−1.35 (m, 9H). ^{13}C NMR (101 MHz, $CDCl_3$): δ 173.0, 172.5, 154.7, 154.0, 79.6, 79.5, 56.6, 56.5, 47.0, 46.8, 37.1, 36.1, 30.5, 29.7, 28.7, 28.5, 24.3, 23.

*(S)-tert-Butyl 2-(Dimethylcarbamothioyl)pyrrolidine-1-carbamate (**47**).* To a solution of **46** (1 equiv) in anhydrous toluene under argon atmosphere was added Lawesson reagent (1.2 equiv). The reaction mixture was warmed at reflux for one night and then evaporated under reduced pressure. Purification by chromatography on silica gel column (AcOEt/hept, 3/7, v/v then 5/5, v/v +1% Et_3N) afforded **47** as a colorless oil (yield 52%). R_f = 0.63 (CH_2Cl_2/MeOH, 95/5). ^{1}H NMR (400 MHz, $CDCl_3$): δ 4.89−4.72 (m, 1 H), 3.72−3.46 (m, 2H), 3.46−3.26 (m, 6H), 2.24−2.08 (m, 2H), 1.86−1.70 (m, 2H), 1.43−1.27 (m, 9H). ^{13}C NMR (101 MHz, $CDCl_3$): δ 206.4, 205.1, 154.7, 153.7, 79.8, 79.7, 62.8, 62.6, 47.2, 47.0, 45.4, 45.2, 41.4, 41.3, 32.7 31.7, 28.8, 28.6, 24.0, 23.5.

*(S)-N,N-Dimethylpyrrolidine-2-carbothioamide, Trifluoroacetate (**48**).* Compound **47** in TFA/CH_2Cl_2 (1/1, v/v) was stirred 30 min at rt and then evaporated and lyophilized to obtain the expected **48** as an oil (quantitative yield). R_f = 0.15 (CH_2Cl_2/MeOH, 9/1). ^{1}H NMR (400 MHz, $CDCl_3$): δ 5.09 (s, 1H), 3.62−3.43 (m, 2H), 3.50 (s, 3H), 3.39 (m, 3H), 2.63−2.49 (m, 1H), 2.21−2.04 (m, 2H), 1.85−1.73 (m, 1H). ^{13}C NMR (101 MHz, $CDCl_3$): δ 197.1, 61.7, 46.9, 46.0, 41.8, 31.9, 25.5.

*(S)-N,N-Dimethylpyrrolidine-2-carboxamide, Trifluoroacetate (**49**).* Compound **46** in TFA/CH_2Cl_2 (1/1, v/v) was stirred 30 min at rt and then evaporated and lyophilized to obtain the expected **49** as an oil (quantitative yield). R_f = 0.15 (CH_2Cl_2/MeOH, 9/1). ^{1}H NMR (400 MHz, $CDCl_3$): δ 4.82 (s, 1H), 3.36−3.52 (m, 2H), 3.02 (s, 3H), 2.98 (s, 3H), 2.41−2.55 (m, 1H), 2.06−2.16 (m, 1H), 1.94−2.04 (m, 1H), 1.82−1.93 (m, 1H). ^{13}C NMR (101 MHz, $CDCl_3$): δ 162.3, 58.1, 46.7, 36.9, 37.4, 29.6, 25.0.

*tert-Butyl (2-(Dimethylamino)-2-oxoethyl)carbamate (**50**).* A solution of Boc-glycine (1 equiv), trimethylamine (2 equiv), and HOBt (1.2 equiv) in CH_2Cl_2 was stirred for 20 min at rt. Dimethylamine hydrochloride (1 equiv) was then added. The mixture was stirred for 20 h at rt. CH_2Cl_2 was then added, and the mixture was washed with 0.3 M aqueous potassium sulfate, saturated aqueous sodium bicarbonate, and brine. The organic phase was dried over Na_2SO_4 and evaporated in vacuo. The expected compound was obtained after purification by chromatography on silica gel column (AcOEt/hept, 1/1, v/v + 1% Et_3N) to afford a colorless oil (yield 46%). R_f = 0.12 (AcOEt/Hept, 1/1). ^{1}H NMR (400 MHz, $CDCl_3$): δ 3.91 (s, 2H), 2.94 (d, 6H, J = 7.9 Hz), 1.41 (s, 9H). ^{13}C NMR (101 MHz, $CDCl_3$): δ 168.5, 156.0, 79.7, 42.5, 36.0, 35.8, 28.6.

*tert-Butyl (2-(Dimethylamino)-2-thioxoethyl)carbamate (**51**).* To a solution of **50** (1 equiv) in anhydrous toluene under argon atmosphere was added Lawesson reagent (1.2 equiv). The reaction mixture was warmed at reflux for one night and then evaporated under reduced pressure. Purification by chromatography on silica gel column (AcOEt/Hept, 5/95, v/v until 60/40, v/v) afforded a colorless oil (yield 63%). R_f = 0.34 (AcOEt/Hept, 1/1). ^{1}H NMR (400 MHz, $CDCl_3$): δ 4.03 (s, 2H), 3.48 (s, 3H), 3.27 (s, 3H), 1.43 (s, 9H). ^{13}C NMR (101 MHz, $CDCl_3$): δ 198.2, 155.7, 79.9, 48.2, 45.0, 40.6, 28.6.

*2-Amino-N,N-dimethylethanethioamide, Trifluoroacetate (**52**).* Compound **51** in TFA/CH_2Cl_2 (1/1, *v/v*) was stirred 30 min at rt and then evaporated and lyophilized to obtain the expected **60** as a white solid (quantitative yield). ^{1}H NMR (400 MHz, CD_3OD): δ 3.99 (s, 2H), 3.49 (s, 3H), 3.33 (s, 3H). ^{13}C NMR (101 MHz, CD_3OD): δ 194.1, 45.7, 45.1, 41.0.

*2-Amino-N,N-dimethylacetamide, Trifluoroacetate (**53**).* Compound **50** in TFA/CH_2Cl_2 (1/1, *v/v*) was stirred 30 min at rt and then evaporated and lyophilized to obtain the expected **53** as a white solid (quantitative yield). MP = 117 °C. ^{1}H NMR (400 MHz, CD_3OD): δ 3.85 (s, 2H), 2.99 (d, 6H, J = 2.2 Hz). ^{13}C NMR (101 MHz, CD_3OD): δ 166.8, 40.9, 36.4, 36.0.

*2-Methyl-4-(1-methyl-1,3a,4,5,10,10a-hexahydrobenzo[b]-pyrazolo[3,4-e][1,4]diazepine-5-carbonyl)benzonitrile (**55**).* $(COCl)_2$ (316 μL, 3.67 mmol, 4 equiv) was added dropwise in a solution of 4-cyano-3-methylbenzoic acid (296 mg, 1.84 mmol, 2 equiv) in anhydrous CH_2Cl_2 (2.5 mL) and few drops of DMF. The mixture was stirred 15 min at 0 °C, 2 h at rt, concentrated, and dried in vacuo. The residue was taken up in anhydrous CH_2Cl_2 (1.8 mL) and added dropwise at 0 °C to a solution of 1-methyl-3*a*,5,10,10*a*-tetrahydrobenzo[*b*]pyrazolo[3,4-*e*][1,4]diazepin-4(1*H*)-one **37** (184 mg, 0.92 mmol, 1 equiv) and triethylamine (256 μL, 1.84 mmol, 2 equiv) in anhydrous CH_2Cl_2 (3.6 mL). The mixture was stirred 30 min at 0 °C and one night at rt. The crude product was taken up in CH_2Cl_2, and the organic phase was washed with saturated aqueous $KHSO_4$. The aqueous phase was extracted with $CHCl_3$/*i*PrOH (8/2, v/v). The organic phases were gathered, washed with saturated aqueous $NaHCO_3$, dried over Na_2SO_4, and evaporated. Purification by chromatography on silica gel column (CH_2Cl_2/MeOH, 95/5, v/v) afforded a beige solid (223 mg; yield 70%). R_f = 0.3 (CH_2Cl_2/MeOH, 95/5). ^{1}H NMR (400 MHz, $CDCl_3$): δ 7.31−7.25 (m, 3H), 7.11 (t, 1H, J = 7.6 Hz), 7.01 (dd, 2H, J = 12.3, 7.6 Hz), 6.68 (dt, 2H, J = 13.8, 6.8 Hz), 5.86 (d, 1H, J = 14.4 Hz), 3.99 (d, 1H, J = 14.4 Hz), 3.85 (s, 3H), 2.39 (s, 3H). ^{13}C NMR (101 MHz, $CDCl_3$): δ 168.0, 142.4, 140.4, 139.8, 138.3, 136.1, 132.0, 130.9, 129.9, 129.3, 125.5, 123.0, 119.5, 114.0, 101.6, 43.5, 35.2, 20.5.

*(4-(Aminomethyl)-3-methylphenyl)(1-methyl-3a,4,10,10a-tetrahydrobenzo[b]pyrazolo[3,4-e][1,4]diazepin-5(1H)-yl)-methanone (**56**).* To a solution of 2-methyl-4-(1-methyl-1,3*a*,4,5,10,10*a*-hexahydrobenzo[*b*]pyrazolo[3,4-*e*][1,4]diazepine-5-carbonyl)benzonitrile **55** (223 mg, 0.64 mmol, 1 equiv) in anhydrous methanol at 0 °C were added cobalt chloride hexahydrate (303 mg, 1.28 mmol, 2 equiv) and sodium borohydride (2.41 g, 6.38 mmol, 10 equiv). The black mixture was stirred for 10 min at 0 °C then 1 h at rt. The mixture was neutralized to pH = 7/8 with a solution of 1 M $KHSO_4$. The methanol was evaporated, and the residue was diluted in a solution of 1 M $KHSO_4$ (15 mL). A precipitate was filtered off and washed with Et_2O. The aqueous phase was extracted with Et_2O and basified up to pH > 10 with a solution of 10 N NaOH. The color switched from pink to blue. The aqueous phase was then extracted with $CHCl_3$. The organic phase was dried over Na_2SO_4 and evaporated in vacuo to afford the expected product as a green powder (180 mg, yield 81%). t_R = 2.41 min. MP = 249 °C. ^{1}H NMR (400 MHz, DMSO-d_6): δ 7.28 (d, 1H, J = 8.0 Hz), 7.17 (s, 1H), 7.15−7.06 (m, 2H), 7.01 (s, 1H), 6.86 (d, 1H, J = 8.0 Hz), 6.75−6.60 (m, 2H), 5.68 (d, 1H, J = 14.7 Hz), 3.88 (d, 1H, J = 14.7 Hz), 3.78 (s, 3H), 3.57 (s, 2H), 2.10 (s, 3H). ^{13}C NMR (101 MHz, DMSO-d_6): δ 168.2, 143.4, 139.8, 138.9, 135.6, 134.6, 130.2, 129.0, 128.1, 125.5, 124.8, 121.2, 119.2, 100.3, 43.1, 42.0, 35.3, 18.3.

*General Method for the Synthesis of Compounds **57**−**61**.* A solution of **56** (1 equiv), carbonyldiimidazole (1.2 equiv), and DIEA (1.5 equiv) in DMF was stirred for 3 h at rt. To this mixture were added one of the amines **48**, **49**, and **52**−**54** (1.3 equiv) and DIEA (2.5 equiv) in DMF. The mixture was stirred overnight at rt and evaporated. Semipreparative HPLC yielded expected compounds **57**−**61**.

*(S)-2-(Dimethylcarbamothioyl)-N-(2-methyl-4-(1-methyl-1,4,5,10-tetrahydrobenzo[b]pyrazolo[3,4-e][1,4]diazepine-5-carbonyl)benzyl)pyrrolidine-1-carboxamide, Trifluoroacetate (**57; LIT-001**).* Prepared from compounds **56** and **48**. White solid (46.7 mg, yield 41%). t_R = 3.32 min. MP = 204 °C. ^{1}H NMR (400 MHz, CD_3OD): δ 7.65 (s, 1H), 7.30 (d, 1H, J = 8 Hz), 7.23−7.14 (m, 2H), 7.06−6.93 (m, 2H), 6.82−6.72 (m, 2H), 5.84 (d, 1H, J = 14.8 Hz), 5.05 (s, 1H), 4.32−4.15 (m, 2H), 3.98 (d, 1H, J = 14.8 Hz), 3.91 (s, 3H), 3.71−3.63 (m, 1H), 3.36 (s, 3H), 3.25 (s, 3H), 2.27−2.16 (m, 1H), 2.09 (s, 3H), 1.97−1.86 (m, 1H), 1.84−1.72 (m, 1H). ^{13}C NMR (101 MHz, CD_3OD): δ 206.1, 171.8, 158.7, 144.6, 141.7, 138.7, 136.4, 135.0, 124.8, 131.5, 130.4, 130.1, 127.4, 127.2, 126.5, 124.4, 121.5, 104.4, 64.4, 47.6, 45.4, 44.3, 42.6, 41.7, 35.1, 32.4, 24.7, 19.0. HPLC t_R = 2.848 min, purity 100% (254 nm). HRMS (EI) calcd for $C_{28}H_{33}N_7O_2S$ $[M + H]^+$ 532.2489, found 532.2473.

DOI: 10.1021/acs.jmedchem.8b00697
J. Med. Chem. 2018, 61, 8670−8692

*(S)-N_2,N_2-Dimethyl-N_1-(2-methyl-4-(1-methyl-1,4,5,10-tetrahydrobenzo[b]pyrazolo[3,4-e][1,4]diazepine-5-carbonyl)-benzyl)pyrrolidine-1,2-dicarboxamide, Trifluoroacetate (**58**).* Prepared from compounds **56** and **49**. White solid (24.1 mg, yield 66%). t_R = 2.99 min. MP = 108.7 °C. ^{1}H NMR (400 MHz, CD_3OD): δ 7.68 (s, 1H), 7.29 (d, H, J = 7.9 Hz), 7.17 (t, 1 H, J = 7.9 Hz), 7.11 (d, 1H, J = 7.9 Hz), 7.06−6.96 (m, 2H), 6.84−6.72 (m, 2H), 5.84 (d, 1H, J = 14.8 Hz), 4.78 (dd, 1H, J = 8.7, 3.8 Hz), 4.32−4.19 (m, 2H), 3.98 (d, 1H, J = 14.8 Hz), 3.58−3.49 (m, 1H), 3.44−3.37 (m, 1H), 3.10 (s, 3H), 2.91 (d, 3H, J = 2.2 Hz), 2.30−2.15 (m, 1H), 2.15 (s, 3H), 2.09−1.93 (m, 2H), 1.79−1.89 (m, 1H). ^{13}C NMR (101 MHz, CD_3OD): δ 175.1, 171.8, 158.9, 144.9, 141.8, 138.8, 136.6, 135.2, 134.8, 134.7, 131.6, 130.6, 130.2, 127.3, 126.6, 124.5, 121.7, 104.8, 58.5, 47.5, 44.3, 42.7, 37.5, 36.4, 35.1, 30.5, 25.5, 19.0. HPLC t_R = 2.549 min, purity 100% (254 nm). HRMS (EI) calcd for $C_{28}H_{33}N_7O_3$ $[M + H]^+$ 516.2717, found 516.2704.

*N,N-Dimethyl-2-(3-(2-methyl-4-(1-methyl-1,4,5,10-tetrahydrobenzo[b]pyrazolo[3,4-e][1,4]diazepine-5-carbonyl)-benzyl)ureido)acetamide Trifluoroacetate (**59**).* Prepared from compounds **56** and **53**. White solid (20.1 mg, yield 65%). t_R = 2.88 min. MP = 112.7 °C. ^{1}H NMR (400 MHz, CD_3OD): δ 7.72 (s, 1H), 7.30 (d, 1H, J = 8.1 Hz), 7.18 (t, 1H, J = 7.6 Hz), 7.07 (d, 1H, J = 7.9 Hz), 7.05 (s, 1H), 6.99 (d, 1H, J = 7.6 Hz), 6.82−6.74 (m, 2H), 5.05 (d, 1H, J = 14.7 Hz), 4.21 (s, 2H), 4.00 (s, 1H), 3.97 (s, 2H), 3.93 (s, 3H), 3.00 (s, 3H), 2.93 (s, 3H), 2.16 (s, 3H). ^{13}C NMR (101 MHz, CD_3OD): δ 171.7, 171.6, 160.9, 141.4, 138.6, 137.0, 135.5, 134.8, 134.5, 131.6, 130.7, 130.2, 127.8, 126.7, 124.6, 121.7, 104.9, 44.3, 42.8, 42.5, 36.5, 36.1, 35.1, 19.0. HPLC t_R = 2.501 min, purity 100% (254 nm). HRMS (EI) calcd for $C_{25}H_{29}N_7O_3$ $[M + H]^+$ 476.2404, found 476.2406.

*N,N-Dimethyl-2-(3-(2-methyl-4-(1-methyl-1,4,5,10-tetrahydrobenzo[b]pyrazolo[3,4-e][1,4]diazepine-5-carbonyl)-benzyl)ureido)ethanethioamide, Trifluoroacetate (**60**).* Prepared from compounds **56** and **52**. White solid (20.6 mg, yield 67%). t_R = 3.12 min. MP = 139 °C. ^{1}H NMR (400 MHz, CD_3OD): δ 7.45 (s, 1H), 7.27 (d, 1H, J = 8 Hz), 7.15 (t, 1H, J = 8 Hz), 7.11 (d, 1H, J = 7.8 Hz), 7.05 (s, 1H), 6.98 (d, 1H, J = 8 Hz), 6.80−6.69 (m, 2H), 5.82 (d, 1H, J = 14.8 Hz), 4.22 (s, 2H), 4.09 (s, 2H), 3.98 (d, 1H, J = 14.8 Hz), 3.89 (s, 3H), 3.47 (s, 3H), 3.13 (t, 1H, J = 5.7 Hz), 2.16 (s, 3H), 1.83−1.65 (m, 2H). ^{13}C NMR (101 MHz, CD_3OD): δ 200.8, 171.8, 160.7, 143.9, 141.3, 139.2, 137.0, 125.7, 134.6, 131.6, 130.7, 130.1, 127.8, 126.6, 124.4, 121.4, 103.9, 45.8, 45.2, 44.5, 42.5, 40.8, 35.3, 23.9, 23.2, 19.0. HPLC t_R = 2.755 min, purity 100% (254 nm). HRMS (EI) calcd for $C_{25}H_{29}N_7O_2S$ $[M + H]^+$ 492.2176, found 492.2163.

*2-(3-(2-Methyl-4-(1-methyl-1,4,5,10-tetrahydrobenzo[b]-pyrazolo[3,4-e][1,4]diazepine-5-carbonyl)benzyl)ureido)methyl acetate, Trifluoroacetate (**61**).* Prepared from compounds **56** and **54**. White solid (20.5 mg, yield 66%). t_R = 2.99 min. MP = 126.8 °C. ^{1}H NMR (400 MHz, CD_3OD): δ 7.68 (s, 1H), 7.33−6.96 (m, 6H), 6.84−6.73 (m, 1H), 5.85 (d, 1H, J = 14.9 Hz), 4.21 (s, 2H), 3.99 (d, 1H, J = 14.9 Hz), 3.92 (s, 3H), 3.86 (s, 2H), 3.72−3.67 (m, 3H), 2.16 (s, 3H). ^{13}C NMR (101 MHz, CD_3OD): δ 173.3, 171.7, 160.9, 141.3, 138.8, 137.0, 135.6, 134.9, 131.6, 130.7, 130.2, 127.8, 126.7, 124.5, 121.6, 104.5, 52.6, 44.4, 42.8, 42.5, 35.1, 18.9. HPLC t_R = 2.601 min, purity 75.88% (254 nm). HRMS (EI) calcd for $C_{24}H_{26}N_6O_4$ $[M + H]^+$ 463.2088, found 463.2078.

Biology: Material and Methods. AVP and OT were purchased from Bachem or Novabiochem, [^{3}H]AVP from Amersham or PerkinElmer Life and Analytical Sciences, BSA from Sigma, and Ro-20-1724 (4-(3-butoxy-4-methoxyphenyl)methyl-2-imidazolidone) from Calbiochem. Synthesized compounds were initially dissolved in DMSO at 10 or 1 μM and then diluted to the desired concentration with the assay buffer.

Cell Culture. Culture of CHO cell lines stably expressing the human vasopressin V_{1a}, V_2, or oxytocin receptors was performed as previously described.[49] Culture of HEK293 cell lines stably expressing V_{1a}, V_2, or OT receptors cell culture was performed as previously described.[88]

Membrane Preparations. To increase the level of expression of some receptors (OT-R, V_{1a}-R), the CHO cells were treated overnight with 5 mM sodium butyrate. As already published, this treatment does not modify the pharmacological properties of the receptors.[89] The membranes were prepared as already described.[49]

Radioligand Binding Assays. Binding assays were performed at 30 °C using [^{3}H]AVP as the radioligand and CHO cells-membrane proteins (10−15 μg for V_{1a} and OT receptors, 5 μg for V_2 receptor), as previously described.[49]

TR-FRET Binding Assay. These assays were performed as described in Zwier et al.[90] Briefly, HEK293 cells stably expressing V_{1a}, V_2, or OT receptors fused to the SNAP-tag suicide enzyme were labeled with the fluorescent donor substrate SNAP-Lumi4-Tb at 100 nM in Tag-lite labeling medium for 1 h at 37 °C. Cells were then washed three times in Tag-lite medium and then incubated with the fluorescent ligands. For competition assays, increasing concentrations of cold competitor ligand in Tag-lite medium were first added to the cells, then a fixed concentration of fluorescent ligand (30 to 50 nM) was added. After 3 h incubation at room temperature, plates were read in an HTRF-compatible multiwell plate reader with a classic HTRF protocol (excitation at 340 nm, donor emission measured at 615 nm and acceptor emission at 665 nm, 50 μs delay, 500 μs integration).

Functional Assays. I. CHO Cells. The functional agonist and competitive antagonist properties of each ligand were determined for the human vasopressin and oxytocin receptors subtypes stably expressed in CHO cells as previously described.[49] The accumulation of *myo*-inositol 1-phosphate (V_{1a} and OT receptors) was determined by the IP-One assay, and the accumulation of cAMP (V_2 receptor) was determined by the cAMP *dynamic 2* assay, both kindly provided by Cisbio International.

ii. HEK Cells. Agonist and antagonist properties of each ligand were determined by measuring intracellular calcium flux. For that, HEK293 cells stably expressing the human vasopressin V_{1a} or oxytocin OT receptors were cultured in flasks up to 80−90% confluence. Then the cells were incubated for 45 min at 37 °C with 5 μM of the fluorescent dye Indo1-AM in Hepes buffer supplemented with 0.1% BSA. After a washing step with PBS buffer, the cells were detached using accutase (PAA), and suspended in Hepes-BSA buffer. Then 200 μL of a 0.5 × 10^6 cells/mL suspension were distributed in each well of a 96-well plate. Fluorescence of Indo1 was recorded at 401 and 475 nm (excitation wavelength at 338 nm) for 3 min following addition of ligand using FlexStation^{III} reader (Molecular Devices).

To test the antagonist effect, fluorescence was recorded in the same way after addition of a mix made with ligand and the endogenous agonist (10 nM OT for OT receptor or 1 nM AVP for V_{1a} receptor). A dose−response curve was generated by plotting normalized fluorescence ratio of Indo1 and ligand concentrations tested. EC_{50} values (for agonist properties) and IC_{50} values (for antagonist properties) were calculated from the dose−response curves, and the maximal responses induced by ligands were expressed as percentages of maximal stimulation by the endogenous agonist.

Signaling Assays. HEK293FT cells (Life Technologies, USA) were grown in complete medium (Dulbecco's Modified Eagle's Medium (DMEM) supplemented with 10% (v/v) fetal bovine serum, 100 U/mL penicillin, 0.1 mg/mL streptomycin, and 1 mM glutamine) (Eurobio, France) at 37 °C in 5% CO_2. For calcium release and BRET1 assays, transient transfections were performed in 6-well and 96-well plates, respectively (Greiner Bio-One, France), using Metafectene PRO (Biontex, München, Germany) and following the manufacturer's protocol.

Regarding the assessment of β-arrestin2 recruitment, BRET1 assays, pcDNA3.1 plasmids encoding the human OT-R, V_{1a}-R, V_{1b}-R, or V_2-R cDNAs tagged at their C-terminus with the luciferase Rluc8 (12.5, 12.5, 25, and 25 ng/well, respectively) and pcDNA3 plasmid encoding *β-Arrestin2*-Venus (75 ng/well) were diluted in 25 μL of non-supplemented DMEM, mixed with 25 μL of a nonsupplemented DMEM-Metafectene PRO (0.5 μL) mixture, incubated for 15−20 min at room temperature and added to the well. Cells (10^5 in 200 μL) in complete medium were then added and incubated for 48 h. After overnight serum depletion, cells were stimulated with dose−responses of the drugs diluted in PBS (1×) containing 5 mM HEPES and 5 μM coelenterazine h (Interchim) and BRET was immediately measured

DOI: 10.1021/acs.jmedchem.8b00697
J. Med. Chem. 2018, 61, 8670−8692

upon drug stimulation for 30 min using the Mithras LB 943 plate reader (Berthold, France).

For calcium assays, cells were plated 1 day prior to transfection with 250 ng/well of Aequorin (luciferase calcium sensor) plasmid and 150 ng/well pcDNA3.1 plasmids encoding the human OT-R, V_{1a}-R, V_{1b}-R, or V_2-R cDNAs (Missouri S&T cDNA Resource Center) diluted in 200 μL of nonsupplemented DMEM-Metafectene PRO (5 μL/well) mixture. After 48 h, cells were incubated 3 h in HBSS without calcium followed by 1 h in HBSS with 1.3 mM calcium, both containing 5 μM of coelenterazine h. Then 40 μL of incubated cells were injected on 10 μL of dose−responses of drugs diluted in HBSS-1.3 mM calcium and calcium release was measured for 20 s using Mithras LB 943 plate reader and, for calcium release normalization, by the addition of ionomycin for 30 s.

For the two assays, cells were stimulated with dose responses of OT, carbetocin, compound **57** and WAY-267464 (from 10^{-5} to 10^{-12} M) and vasopressin at 10^{-5} M, or dose−responses of compound **57** in the presence of AVP (at EC_{80}) or Pfizer's OT antagonist PF 3274167[91,92] in the presence of compound **57** (at EC_{80}). All reference compounds were purchased at Tocris Bioscience and diluted at 10^{-2} M stock solution in DMSO. The area under the curves for the two assays (480 nm/540 nm BRET ratio for β-arrestin recruitment and luciferase arbitrary units for calcium assay) were plotted and analyzed using GraphPad Prism 7 software. A representative graph was presented from at least three independent experiments.

In Vivo Assays. (i) *Animals*: Male and female *Oprm1*$^{+/+}$ and *Oprm1*$^{-/-}$ were bred in house on a 50% 129SVPas−50% C57BL/6J hybrid background, group-housed, and maintained on a 12 h light/dark cycle at controlled temperature (21 ± 1 °C) with food and water ad libitum. *Oprm1*$^{+/+}$ and *Oprm1*$^{-/-}$ pups were bred from homozygous parents, as we previously showed that parental care has no influence on behavioral phenotype in these animals (cross-fostering experiments[73]). All experimental procedures were conducted in accordance with the European Communities Council Directive 2010/63/EU and approved by the Comité d'Ethique en Expérimentation Animale Val de Loire (C2EA-19, APAFIS no. 3086-20l5120813572006 v5). (ii) *Drugs*: Compound **57** was dissolved in carboxymethyl cellulose (CMC, 1%)−NaCl (0.9%) as a vehicle solution and administered at the dose of 10 or 20 mg/kg. Compound **57** or vehicle were injected intraperitoneally to the animals 30 min before testing in a volume of 10 mL/kg. (iii) *Behavioral testing*: Naïve male and female animals aged 8−10 weeks were used in each experimental group (n = 4 per sex and genotype). The direct social interaction test was performed in four equal square areas (50 cm × 50 cm) separated by 35 cm high opaque white plastic walls over a white Plexiglas platform (infrared floor, View Point, France) covered with a black plastic floor (transparent to infrared). An assay begun when a pair of unfamiliar (not cage mates) age-, sex-, genotype-, and treatment-matched mice was introduced in each arena for 10 min (15 lx). The amount of time spent in nose contacts (NCs), the number and duration of these contacts, the number of following episodes, and the number of grooming episodes occurring immediately (<5 s) after a social contact (nose or paw contact) were scored a posteriori on video recordings (infrared light-sensitive video camera) using an ethological keyboard (Labwatcher, View Point, France) by a trained experimenter and blind to experimental conditions.[73]

Brain Penetration. Brain penetration of compound **57** was studied in CD-1 mice. A 1 mg/mL solution of compound **57** in 0.5% carboxymethylcellulose/0.9% NaCl solution was prepared. Volumes of 10 mL/kg (10 mg/kg) were administered intraperitonally to 12 mice. Three mice were sacrified at the end of each time period after 15, 45, 90, or 240 min. Blood was collected and plasma was separated by centrifugation. Brains were collected after perfusion of animals with a 3 mM EDTA/0.9% NaCl solution. Samples were frozen and stored at −80 °C before treatment. Plasma samples (400 μL) were mixed with acetonitrile to precipitate and discard proteins (15000g centrifugation for 5 min at 16 °C). The supernatants were analyzed by UHPLC-MS/MS (Shimadzu LC-MS 8030). Brains were homogenized in 400 μL of water, then treated with 800 μL of acetonitrile and analyzed in the same way as plasma samples. Two samples from nontreated mice were analyzed in parallel as controls.

■ ASSOCIATED CONTENT

Supporting Information

The Supporting Information is available free of charge on the ACS Publications website at DOI: 10.1021/acs.jmedchem.8b00697.

Synthesis of precursor compounds **1**−**8**, **28**, **31**, **37**; signaling data for compound **57** (PDF)

Molecular formula strings (CSV)

■ AUTHOR INFORMATION

Corresponding Author

*Phone: +33 (0)3 68 85 42 32. Fax: +33 (0)3 68 85 43 10. E-mail: mhibert@unistra.fr.

ORCID

Pascal Villa: 0000-0003-3466-4852

Dominique Bonnet: 0000-0002-8252-9199

Marcel Hibert: 0000-0001-7786-7276

Author Contributions

#M.-C.F., L.P.P., E.P., and S.L. contributed equally to this work.

Notes

The authors declare no competing financial interest.

■ ACKNOWLEDGMENTS

This work was supported by research grants from the Centre National de la Recherche Scientifique (CNRS−Mission Interdisciplinaire, programme ITMM), the Université de Strasbourg, the LabEx Medalis (Programme Investissement d'Avenir: grant ANR-10-LABX-0034), the French government under the specific ANR-14-CE16-0005-01 project (OT-ism), Région Centre (ARD2020 Biomédicament−GPCRAb), and the LabEx MabImprove (Tours—Montpellier). This work was performed thanks to the Plateforme Arpège of Montpellier. HTRF and Tag-lite are registered trademarks of Cisbio Bioassays. Lumi4 is a registered trademark of Lumiphore, Inc. SNAP-tag is a trademark of New England Biolabs, Inc. We thank Cyril Antheaume, Barbara Schaeffer, and Justine Vieville for NMR experiments and experiments and Pascale Buisine and Patrick Wehrung for mass spectrometry (PACSI platform, GDS3670). We are also grateful to Sophie Gioria for some in vitro pharmacological studies (PCBIS, UMS3286). We thank the Experimental Unit PAO-1297 (EU0028) from the INRA−Val de Loire Centre for animal breeding and care. L.P. Pellissier acknowledges postdoctoral support from the Marie-Curie/AgreenSkills Program.

■ ABBREVIATION USED

ASD, autism spectrum disorder; ATR, attenuated total reflection; AVP, arginine-vasopressin; BSA, bovine serum albumin; ^{13}C NMR, carbon 13 nuclear magnetic resonance; CDI, carbonyldiimidazole; cAMP, cyclic adenosine 5′-monophosphate; CHO, Chinese hamster ovary; CNS, central nervous system; DIEA, diisopropylethylamine; DMAP, *N*,*N*-dimethyl-4-aminopyridine; DMF, dimethylformamide; DMSO, dimethyl sulfoxide; EDCI, 1-ethyl-3-(3-(dimethylamino)propyl)-carbodiimide; ESI-TOF, electron spray ionization-time-of-flight; FRET, fluorescence resonance energy transfer; hept, heptane; GPCR, G protein-coupled receptors; HOBt, *N*-hydroxybenzotriazole; ^{1}H NMR, proton nuclear magnetic resonance; HTRF, homogeneous time-resolved fluorescence; HRMS, high resolution mass spectrometry; i.n., intranasal; IP, inositol phosphate; ip, intraperitoneal; iv, intravenous; *J*,

DOI: 10.1021/acs.jmedchem.8b00697
J. Med. Chem. 2018, 61, 8670−8692

coupling constant; NMP, *N*-methyl-2-pyrrolidone; OT, oxytocin; OT-R, oxytocin receptor; PET, positron emission tomography; R_f, retention factor; RP-HPLC, reverse-phase high performance liquid chromatography; rt, room temperature; SAR, structure−activity relashionships; SEM, standard error of the mean; TFA, trifluoroacetic acid; THF, tetrahydrofuranne; TLC, thin layer chromatography; Tris, 2-amino-2-hydroxymethyl-1,3-propanediol; V_{1a}-R, vasopressin V_{1a} receptor; V_{1b}-R, vasopressin V_{1b} receptor; V_2-R, vasopressin V_2 receptor

REFERENCES

(1) Doernberg, E.; Hollander, E. Neurodevelopmental disorders (ASD and ADHD): DSM-5, ICD-10, and ICD-11. *CNS Spectrums* **2016**, *21*, 295−299.

(2) Centers for Disease Control and Prevention. Prevalence of autism spectrum disorders—Autism and developmental disabilities monitoring network, 14 sites, United States, 2008. *MMWR Surveill. Summ.* **2012**, *61*, 1−19.

(3) Vorstman, J. A. S.; Parr, J. R.; Moreno-De-Luca, D.; Anney, R. J. L.; Nurnberger, J. I., Jr.; Hallmayer, J. F. Autism genetics: opportunities and challenges for clinical translation. *Nat. Rev. Genet.* **2017**, *18*, 362−376.

(4) de la Torre-Ubieta, L.; Won, H.; Stein, J. L.; Geschwind, D. H. Advancing the understanding of autism disease mechanisms through genetics. *Nat. Med.* **2016**, *22*, 345−361.

(5) Krishnan, A.; Zhang, R.; Yao, V.; Theesfeld, C. L.; Wong, A. K.; Tadych, A.; Volfovsky, N.; Packer, A.; Lash, A.; Troyanskaya, O. G. Genome-wide prediction and functional characterization of the genetic basis of autism spectrum disorder. *Nat. Neurosci.* **2016**, *19*, 1454−1462.

(6) Kazdoba, T. M.; Leach, P. T.; Yang, M.; Silverman, J. L.; Solomon, M.; Crawley, J. N. Translational mouse models of autism: advancing toward pharmacological therapeutics. *Curr. Top. Behav. Neurosci.* **2015**, *28*, 1−52.

(7) Argyropoulos, A.; Gilby, K. L.; Hill-Yardin, E. L. Studying autism in rodent models: reconciling endophenotypes with comorbidities. *Front. Hum. Neurosci.* **2013**, *7*, 417.

(8) Leigh, J. P.; Du, J. Brief report: forecasting the economic burden of autism in 2015 and 2025 in the United States. *J. Autism Dev. Disord.* **2015**, *45*, 4135−4139.

(9) Jacquemont, S.; Curie, A.; des Portes, V.; Torrioli, M. G.; Berry-Kravis, E.; Hagerman, R. J.; Ramos, F. J.; Cornish, K.; He, Y.; Paulding, C.; Neri, G.; Chen, F.; Hadjikhani, N.; Martinet, D.; Meyer, J.; Beckmann, J. S.; Delange, K.; Brun, A.; Bussy, G.; Gasparini, F.; Hilse, T.; Floesser, A.; Branson, J.; Bilbe, G.; Johns, D.; Gomez-Mancilla, B. Epigenetic modification of the FMR1 gene in fragile X syndrome is associated with differential response to the mGluR5 antagonist AFQ056. *Sci. Transl. Med.* **2011**, *3*, 64ra1.

(10) Frye, R. E. Clinical potential, safety, and tolerability of arbaclofen in the treatment of autism spectrum disorder. *Drug, Healthcare Patient Saf.* **2014**, *10*, 69−76.

(11) Lemonnier, E.; Villeneuve, N.; Sonie, S.; Serret, S.; Rosier, A.; Roue, M.; Brosset, P.; Viellard, M.; Bernoux, D.; Rondeau, S.; Thummler, S.; Ravel, D.; Ben-Ari, Y. Effects of bumetanide on neurobehavioral function in children and adolescents with autism spectrum disorders. *Transl. Psychiatry* **2017**, *7*, e1056.

(12) Tyzio, R.; Nardou, R.; Ferrari, D. C.; Tsintsadze, T.; Shahrokhi, A.; Eftekhari, S.; Khalilov, I.; Tsintsadze, V.; Brouchoud, C.; Chazal, G.; Lemonnier, E.; Lozovaya, N.; Burnashev, N.; Ben-Ari, Y. Oxytocin-mediated GABA inhibition during delivery attenuates autism pathogenesis in rodent offspring. *Science* **2014**, *343*, 675−679.

(13) Hollander, E.; Novotny, S.; Hanratty, M.; Yaffe, R.; DeCaria, C. M.; Aronowitz, B. R.; Mosovich, S. Oxytocin infusion reduces repetitive behaviors in adults with autistic and Asperger's disorders. *Neuropsychopharmacology* **2003**, *28*, 193−198.

(14) Hollander, E.; Bartz, J.; Chaplin, W.; Phillips, A.; Sumner, J.; Soorya, L.; Anagnostou, E.; Wasserman, S. Oxytocin increases retention of social cognition in autism. *Biol. Psychiatry* **2007**, *61*, 498−550.

(15) Andari, E.; Duhamel, J. R.; Zalla, T.; Herbrecht, E.; Leboyer, M.; Sirigu, A. Promoting social behavior with oxytocin in high-functioning autism spectrum disorders. *Proc. Natl. Acad. Sci. U. S. A.* **2010**, *107*, 4389−4394.

(16) Guastella, A. J.; Einfeld, S. L.; Gray, K. M.; Rinehart, N. J.; Tonge, B. J.; Lambert, T. J.; Hickie, I. B. Intranasal oxytocin improves emotion recognition for youth with autism spectrum disorders. *Biol. Psychiatry* **2010**, *67*, 692−694.

(17) Kosaka, H.; Munesue, T.; Ishitobi, M.; Asano, M.; Omori, M.; Sato, M.; Tomoda, A.; Wada, Y. Long-term oxytocin administration improves social behaviors in a girl with autistic disorder. *BMC Psychiatry* **2012**, *12*, 110.

(18) Anagnostou, E.; Soorya, L.; Brian, J.; Dupuis, A.; Mankad, D.; Smile, S.; Jacob, S. Intranasal oxytocin in the treatment of autism spectrum disorders: a review of literature and early safety and efficacy data in youth. *Brain Res.* **2014**, *1580*, 188−198.

(19) Tachibana, M.; Kagitani-Shimono, K.; Mohri, I.; Yamamoto, T.; Sanefuji, W.; Nakamura, A.; Oishi, M.; Kimura, T.; Onaka, T.; Ozono, K.; Taniike, M. Long-term administration of intranasal oxytocin is a safe and promising therapy for early adolescent boys with autism spectrum disorders. *J. Child Adolesc. Psychopharmacol.* **2013**, *23*, 123−127.

(20) Dadds, M. R.; Macdonald, E.; Cauchi, A.; Williams, K.; Levy, F.; Brennan, J. Nasal oxytocin for social deficits in childhood autism: a randomized controlled trial. *J. Autism Dev. Disord.* **2014**, *44*, 521−531.

(21) MacDonald, E.; Dadds, M. R.; Brennan, J. L.; Williams, K.; Levy, F.; Cauchi, A. J. A review of safety, side-effects and subjective reactions to intranasal oxytocin in human research. *Psychoneuroendocrinology* **2011**, *36*, 1114−1126.

(22) Althaus, M.; Groen, Y.; Wijers, A. A.; Noltes, H.; Tucha, O.; Hoekstra, P. J. Oxytocin enhances orienting to social information in a selective group of high-functioning male adults with autism spectrum disorder. *Neuropsychologia* **2015**, *79*, 53−69.

(23) Andari, E.; Richard, N.; Leboyer, M.; Sirigu, A. Adaptive coding of the value of social cues with oxytocin, an fMRI study in autism spectrum disorder. *Cortex* **2016**, *76*, 79−88.

(24) Aoki, Y.; Yahata, N.; Watanabe, T.; Takano, Y.; Kawakubo, Y.; Kuwabara, H.; Iwashiro, N.; Natsubori, T.; Inoue, H.; Suga, M.; Takao, H.; Sasaki, H.; Gonoi, W.; Kunimatsu, A.; Kasai, K.; Yamasue, H. Oxytocin improves behavioural and neural deficits in inferring others' social emotions in autism. *Brain* **2014**, *137*, 3073−3086.

(25) Aoki, Y.; Watanabe, T.; Abe, O.; Kuwabara, H.; Yahata, N.; Takano, Y.; Iwashiro, N.; Natsubori, T.; Takao, H.; Kawakubo, Y.; Kasai, K.; Yamasue, H. Oxytocin's neurochemical effects in the medial prefrontal cortex underlie recovery of task-specific brain activity in autism: a randomized controlled trial. *Mol. Psychiatry* **2015**, *20*, 447−453.

(26) Auyeung, B.; Lombardo, M. V.; Heinrichs, M.; Chakrabarti, B.; Sule, A.; Deakin, J. B.; Bethlehem, R. A. I.; Dickens, L.; Mooney, N.; Sipple, J. A. N.; Thiemann, P.; Baron-Cohen, S. Oxytocin increases eye contact during a real-time, naturalistic social interaction in males with and without autism. *Transl. Psychiatry* **2015**, *5*, e507.

(27) Domes, G.; Heinrichs, M.; Kumbier, E.; Grossmann, A.; Hauenstein, K.; Herpertz, S. C. Effects of intranasal oxytocin on the neural basis of face processing in autism spectrum disorder. *Biol. Psychiatry* **2013**, *74*, 164−171.

(28) Domes, G.; Kumbier, E.; Heinrichs, M.; Herpertz, S. C. Oxytocin promotes facial emotion recognition and amygdala reactivity in adults with Asperger syndrome. *Neuropsychopharmacology* **2014**, *39*, 698−706.

(29) Gordon, I.; Vander Wyk, B. C.; Bennett, R. H.; Cordeaux, C. O.; Lucas, M. V.; Eilbott, J. A.; Zagoory-Sharon, O.; Leckman, J. F.; Feldman, R.; Pelphrey, K. A. Oxytocin enhances brain function in children with autism. *Proc. Natl. Acad. Sci. U. S. A.* **2013**, *110*, 20953−20958.

(30) Kanat, M.; Spenthof, I.; Riedel, A.; van Elst, L. T.; Heinrichs, M.; Domes, G. Restoring effects of oxytocin on the attentional preference for faces in autism. *Transl. Psychiatry* **2017**, *7*, e1097.

(31) Watanabe, T.; Kuroda, M.; Kuwabara, H.; Aoki, Y.; Iwashiro, N.; Tatsunobu, N.; Takao, H.; Nippashi, Y.; Kawakubo, Y.; Kunimatsu, A.;

DOI: 10.1021/acs.jmedchem.8b00697
J. Med. Chem. 2018, 61, 8670−8692

Kasai, K.; Yamasue, H. Clinical and neural effects of six-week administration of oxytocin on core symptoms of autism. *Brain* **2015**, *138*, 3400−3412.
(32) Yatawara, C. J.; Einfeld, S. L.; Hickie, I. B.; Davenport, T. A.; Guastella, A. J. The effect of oxytocin nasal spray on social interaction deficits observed in young children with autism: a randomized clinical crossover trial. *Mol. Psychiatry* **2016**, *21*, 1225−1231.
(33) Preckel, K.; Kanske, P.; Singer, T.; Paulus, F. M.; Krach, S. Clinical trial of modulatory effects of oxytocin treatment on higher-order social cognition in autism spectrum disorder: a randomized, placebo-controlled, double-blind and crossover trial. *BMC Psychiatry* **2016**, *16*, 329.
(34) Quintana, D. S.; Alvares, G. A.; Hickie, I. B.; Guastella, A. J. Do delivery routes of intranasally administered oxytocin account for observed effects on social cognition and behavior? A two-level model. *Neurosci. Biobehav. Rev.* **2015**, *49*, 182−192.
(35) Munesue, T.; Nakamura, H.; Kikuchi, M.; Miura, Y.; Takeuchi, N.; Anme, T.; Nanba, E.; Adachi, K.; Tsubouchi, K.; Sai, Y.; Miyamoto, K.; Horike, S.; Yokoyama, S.; Nakatani, H.; Niida, Y.; Kosaka, H.; Minabe, Y.; Higashida, H. Oxytocin for male subjects with autism spectrum disorder and comorbid intellectual disabilities: a randomized pilot study. *Front. Psychiatry* **2016**, *7*, 2.
(36) Lacivita, E.; Perrone, R.; Margari, L.; Leopoldo, M. Targets for drug therapy for autism spectrum disorder: challenges and future directions. *J. Med. Chem.* **2017**, *60*, 9114−9141.
(37) Wenzel, B.; Mollitor, J.; Deuther-Conrad, W.; Dukic-Stefanovic, S.; Kranz, M.; Vraka, C.; Teodoro, R.; Günther, R.; Donat, C. K.; Ludwig, F.; Fischer, S.; Smits, R.; Wadsak, W.; Mitterhauser, M.; Steinbach, J.; Hoepping, A.; Brust, P. Development of a novel nonpeptidic (18)F-labeled radiotracer for in vivo imaging of oxytocin receptors with positron emission tomography. *J. Med. Chem.* **2016**, *59*, 1800−1817.
(38) Marzano, C.; Jakobsen, S.; Salinas, C.; Tang, S. P.; Bender, D.; Passchier, J.; Plisson, C. J. Radiosynthesis and evaluation of 1-substituted 3-(2,3-dihydro-1H-inden-2-yl)-6-(1-ethylpropyl)-(3R,6R)-2,5-piperazinedione derivatives as PET tracers for imaging the central oxytocinergic system. *J. Labelled Compd. Radiopharm.* **2017**, *60*, 556−565.
(39) Gimpl, G. Oxytocin receptor ligands: a survey of the patent literature. *Expert Opin. Ther. Pat.* **2008**, *18*, 1239−1251.
(40) Ring, R. H.; Schechter, L. E.; Leonard, S. K.; Dwyer, J. M.; Platt, B. J.; Graf, R.; Grauer, S.; Pulicicchio, C.; Resnick, L.; Rahman, Z.; Sukoff Rizzo, S. J.; Luo, B.; Beyer, C. E.; Logue, S. F.; Marquis, K. L.; Hughes, Z. A.; Rosenzweig-Lipson, S. Receptor and behavioral pharmacology of WAY-267464, a non-peptide oxytocin receptor agonist. *Neuropharmacology* **2010**, *58*, 69−77.
(41) Gossen, A.; Hahn, A.; Westphal, L.; Prinz, S.; Schultz, R. T.; Gründer, G.; Spreckelmeyer, K. N. Oxytocin plasma concentrations after single intranasal oxytocin administration - a study in healthy men. *Neuropeptides* **2012**, *46*, 211−215.
(42) Guastella, A. J.; Hickie, I. B.; McGuinness, M. M.; Otis, M.; Woods, E. A.; Disinger, H. M.; Chan, H. K.; Chen, T. F.; Banati, R. B. Recommendations for the standardisation of oxytocin nasal administration and guidelines for its reporting in human research. *Psychoneuroendocrinology* **2013**, *38*, 612−625.
(43) Busnelli, M.; Chini, B. Molecular basis of oxytocin receptor signaling in the brain: what we know and what we need to know. *Curr. Top. Behav. Neurosci.* **2017**, *35*, 3−29.
(44) Grinevich, V.; Knobloch-Bollmann, H. S.; Eliava, M.; Busnelli, M.; Chini, B. Assembling the puzzle: pathways of oxytocin signaling in the brain. *Biol. Psychiatry* **2016**, *79*, 155−164.
(45) Sala, M.; Braida, D.; Lentini, D.; Busnelli, M.; Bulgheroni, E.; Capurro, V.; Finardi, A.; Donzelli, A.; Pattini, L.; Rubino, T.; Parolaro, D.; Nishimori, K.; Parenti, M.; Chini, B. Pharmacologic rescue of impaired cognitive flexibility, social deficits, increased aggression, and seizure susceptibility in oxytocin receptor null mice: a neurobehavioral model of autism. *Biol. Psychiatry* **2011**, *69*, 875−882.
(46) Wiśniewski, K.; Alagarsamy, S.; Galyean, R.; Tariga, H.; Thompson, D.; Ly, B.; Wiśniewska, H.; Qi, S.; Croston, G.; Laporte, R.; Rivière, P. J.; Schteingart, C. D. New, potent, and selective peptidic oxytocin receptor agonists. *J. Med. Chem.* **2014**, *57*, 5306−5317.
(47) Adachi, Y.; Sakimura, K.; Shimizu, Y.; Nakayama, M.; Terao, Y.; Yano, T.; Asami, T. Potent and selective oxytocin receptor agonists without disulfide bridges. *Bioorg. Med. Chem. Lett.* **2017**, *27*, 2331−2335.
(48) Pitt, G. R.; Batt, A. R.; Haigh, R. M.; Penson, A. M.; Robson, P. A.; Rooker, D. P.; Tartar, A. L.; Trim, J. E.; Yea, C. M.; Roe, M. B. Non-peptide oxytocin agonists. *Bioorg. Med. Chem. Lett.* **2004**, *14*, 4585−4589.
(49) Frantz, M. C.; Rodrigo, J.; Boudier, L.; Durroux, T.; Mouillac, B.; Hibert, M. Subtlety of the structure-affinity and structure-efficacy relationships around a nonpeptide oxytocin receptor agonist. *J. Med. Chem.* **2010**, *53*, 1546−1562.
(50) Olszewski, P. K.; Ulrich, C.; Ling, N.; Allen, K.; Levine, A. S. A non-peptide oxytocin receptor agonist, WAY-267,464, alleviates novelty-induced hypophagia in mice: insights into changes in c-Fos immunoreactivity. *Pharmacol., Biochem. Behav.* **2014**, *124*, 367−372.
(51) Hicks, C.; Jorgensen, W.; Brown, C.; Fardell, J.; Koehbach, J.; Gruber, C. W.; Kassiou, M.; Hunt, G. E.; McGregor, I. S. The nonpeptide oxytocin receptor agonist WAY 267,464: receptor-binding profile, prosocial effects and distribution of c-Fos expression in adolescent rats. *J. Neuroendocrinol.* **2012**, *24*, 1012−1029.
(52) Weill, N.; Valencia, C.; Gioria, S.; Villa, P.; Hibert, M.; Rognan, D. Identification of non peptide Oxytocin receptor ligands by receptor-ligand fingerprint similarity research. *Mol. Inf.* **2011**, *30*, 521−526.
(53) Bissantz, C.; Logean, A.; Rognan, D. High-throughput modeling of human G-protein coupled receptors: amino acid sequence alignment, three-dimensional model building, and receptor library screening. *J. Chem. Inf. Comput. Sci.* **2004**, *44*, 1162−1176.
(54) Tahara, A.; Tomura, Y.; Wada, K.; Kusayama, T.; Tsukada, J.; Takanashi, M.; Yatsu, T.; Uchida, W.; Tanaka, A. Pharmacological profile of YM087, a novel potent nonpeptide vasopressin V1a and V2 receptor antagonist, in vitro and in vivo. *J. Pharmacol. Exp. Ther.* **1997**, *282*, 301−308.
(55) Tahara, A.; Tsukada, J.; Tomura, Y.; Kusayama, T.; Wada, K.; Ishii, N.; Taniguchi, N.; Suzuki, T.; Yatsu, T.; Uchida, W.; Shibasaki, M. Effects of YM218, a nonpeptide vasopressin V1A receptor-selective antagonist, on human vasopressin and oxytocin receptors. *Pharmacol. Res.* **2005**, *51*, 275−281.
(56) Xiang, M. A.; Rybczynski, P. J.; Patel, M.; Chen, R. H.; McComsey, D. F.; Zhang, H. C.; Gunnet, J. W.; Look, R.; Wang, Y.; Minor, L. K.; Zhong, H. M.; Villani, F. J.; Demarest, K. T.; Damiano, B. P.; Maryanoff, B. E. Next-generation spirobenzazepines: identification of RWJ-676070 as a balanced vasopressin V1a/V2 receptor antagonist for human clinical studies. *Bioorg. Med. Chem. Lett.* **2007**, *17*, 6623−6628.
(57) Nakamura, S.; Yamamura, Y.; Itoh, S.; Hirano, T.; Tsujimae, K.; Aoyama, M.; Kondo, K.; Ogawa, H.; Shinohara, T.; Kan, K.; Tanada, Y.; Teramoto, S.; Sumida, T.; Nakayama, S.; Sekiguchi, K.; Kambe, T.; Tsujimoto, G.; Mori, T.; Tominaga, M. Characterization of a novel nonpeptide vasopressin V2-agonist, OPC-51803, in cells transfected human vasopressin receptor subtypes. *Br. J. Pharmacol.* **2000**, *129*, 1700−1706.
(58) Matsuhisa, A.; Tanaka, A.; Kikuchi, K.; Shimada, Y.; Yatsu, T.; Yanagisawa, I. Nonpeptide arginine vasopressin antagonists for both V1a and V2 receptors: synthesis and pharmacological properties of 2-phenyl-4′-[(2,3,4,5-tetrahydro-1H-1-benzazepin-1-yl)carbonyl]-benzanilide derivatives. *Chem. Pharm. Bull.* **1997**, *45*, 1870−1874.
(59) Kondo, K.; Ogawa, H.; Shinohara, T.; Kurimura, M.; Tanada, Y.; Kan, K.; Yamashita, H.; Nakamura, S.; Hirano, T.; Yamamura, Y.; Mori, T.; Tominaga, M.; Itai, A. Novel design of nonpeptide AVP V2 receptor agonists: structural requirements for an agonist having 1-(4-amino-benzoyl)-2,3,4,5-tetrahydro-1H-1-benzazepine as a template. *J. Med. Chem.* **2000**, *43*, 4388−4397.
(60) Caggiano, T. J. WAY-VNA-932. Treatment of central diabetes insipidus, treatment of nocturnal enuresis, treatment of nocturia, vasopressin V2 agonist. *Drugs Future* **2002**, *27*, 248−253.

DOI: 10.1021/acs.jmedchem.8b00697
J. Med. Chem. 2018, 61, 8670−8692

(61) Failli, A. A.; Shumsky, J. S.; Steffan, R. J.; Caggiano, T. J.; Williams, D. K.; Trybulski, E. J.; Ning, X.; Lock, Y.; Tanikella, T.; Hartmann, D.; Chan, P. S.; Park, C. H. Pyridobenzodiazepines: a novel class of orally active, vasopressin V2 receptor selective agonists. *Bioorg. Med. Chem. Lett.* **2006**, *16*, 954−959.
(62) Gong, Y.; Pauls, H. W. A convenient synthesis of heteroaryl benzoic acids via Suzuki reaction. *Synlett.* **2000**, *6*, 829−831.
(63) Sasatani, S.; Miyazaki, T.; Maruoka, K.; Yamamoto, H. Diisobutylaluminium hydride: a novel reagent for the reduction of oximes. *Tetrahedron Lett.* **1983**, *24*, 4711−4712.
(64) Kondo, K.; Ogawa, H.; Yamashita, H.; Miyamoto, H.; Tanaka, M.; Nakaya, K.; Kitano, K.; Yamamura, Y.; Nakamura, S.; Onogawa, T.; Mori, T.; Tominaga, M. 7-chloro-5-hydroxy-1-[2-methyl-4-(2-methylbenzoyl-amino)benzoyl]-2,3,4,5-tetrahydro-1H-1-benzazepine (OPC-41061): a potent, orally active nonpeptide arginine vasopressin V2 receptor antagonist. *Bioorg. Med. Chem.* **1999**, *7*, 1743−1754.
(65) Ogawa, H.; Yamashita, H.; Kondo, K.; Yamamura, Y.; Miyamoto, H.; Kan, K.; Kitano, K.; Tanaka, M.; Nakaya, K.; Nakamura, S.; Mori, T.; Tominaga, M.; Yabuuchi, Y. Orally active, nonpeptide vasopressin V2 receptor antagonists: a novel series of 1-[4-(benzoylamino)-benzoyl]-2,3,4,5-tetrahydro-1H-benzazepines and related compounds. *J. Med. Chem.* **1996**, *39*, 3547−3555.
(66) Miller, R. J.; Kuliopulos, A.; Coward, J. K. Alkyltransferase model reactions: synthesis of sulfonium and ammonium compounds containing neighboring nucleophiles. Kinetic studies of the intramolecular reaction of amino, hydroxy, phenoxy, and mercapto onium salts. *J. Org. Chem.* **1989**, *54*, 3436−3448.
(67) Proctor, G. R. Azabenzocycloheptenones. Part III. 2,3,4,5-Tetrahydro-5-oxo-1-toluene-p-sulphonylbenz[b]azepine. *J. Chem. Soc.* **1961**, 3989−3994.
(68) Boeglin, D.; Bonnet, D.; Hibert, M. Solid-phase preparation of a pilot library derived from the 2,3,4,5-tetrahydro-1H-benzo[b]azepin-5-amine scaffold. *J. Comb. Chem.* **2007**, *9*, 487−500.
(69) Artico, M.; De Martino, G.; Filacchioni, G.; Giuliano, R. Ricerche su sostanze ad attivita' antiblastica. *Il Farmaco − Ed. Sc.* **1969**, *24*, 276−284.
(70) Caggiano, T. J. WAY-VNA-932. *Drugs Future* **2002**, *27*, 248−253.
(71) Karpenko, I. A.; Margathe, J. F.; Rodriguez, T.; Pflimlin, E.; Dupuis, E.; Hibert, M.; Durroux, T.; Bonnet, D. Selective nonpeptidic fluorescent ligands for oxytocin receptor: design, synthesis, and application to time-resolved FRET binding assay. *J. Med. Chem.* **2015**, *58*, 2547−2552.
(72) Borthwick, A. D. Oral oxytocin antagonists. *J. Med. Chem.* **2010**, *53*, 6525−6538.
(73) Becker, J. A.; Clesse, D.; Spiegelhalter, C.; Schwab, Y.; Le Merrer, J.; Kieffer, B. L. Autistic-like syndrome in mu opioid receptor null mice is relieved by facilitated mGluR4 activity. *Neuropsychopharmacology* **2014**, *39*, 2049−2060.
(74) Moles, A.; Kieffer, B. L.; D'Amato, F. R. Deficit in attachment behavior in mice lacking the mu-opioid receptor gene. *Science* **2004**, *304*, 1983−1986.
(75) Pellissier, L. P.; Gandía, J.; Laboute, T.; Becker, J. A.; Le Merrer, J. μ opioid receptor, social behaviour and autism spectrum disorder: reward matters. *Br. J. Pharmacol.* **2018**, *175*, 2750−2769.
(76) Dölen, G.; Darvishzadeh, A.; Huang, K. W.; Malenka, R. C. Social reward requires coordinated activity of nucleus accumbens oxytocin and serotonin. *Nature* **2013**, *501*, 179−184.
(77) Gigliucci, V.; Leonzino, M.; Busnelli, M.; Luchetti, A.; Palladino, V. S.; D'Amato, F. R.; Chini, B. Region specific up-regulation of oxytocin receptors in the opioid oprm1 (−/−) mouse model of autism. *Front Pediatr.* **2014**, *2*, 91.
(78) Jorgensen, W. T.; Gulliver, D.; Werry, E. L.; Reekie, T.; Connor, M.; Kassiou, M. Flexible analogues of WAY-267,464: Synthesis and pharmacology at the human oxytocin and vasopressin 1a receptors. *Eur. J. Med. Chem.* **2016**, *108*, 730−740.
(79) Hou, T. J.; Xu, X. J. ADME evaluation in drug discovery. 3. Modeling blood-brain barrier partitioning using simple molecular descriptors. *J. Chem. Inf. Comput. Sci.* **2003**, *43*, 2137−2152.
(80) *MarvinSketch 6.0.0*; ChemAxon Software, 2013.
(81) GTEx Consortium. The genotype-tissue expression (GTEx) pilot analysis: multitissue gene regulation in humans. *Science* **2015**, *348*, 648−660.
(82) Lindsay, S. J.; Xu, Y.; Lisgo, S. N.; Harkin, L. F.; Copp, A. J.; Gerrelli, D.; Clowry, G. J.; Talbot, A.; Keogh, M. J.; Coxhead, J.; Santibanez-Koref, M.; Chinnery, P. F. HDBR expression: a unique resource for global and individual gene expression studies during early human brain development. *Front. Neuroanat.* **2016**, *10*, 86.
(83) Goldsmith, S. R.; Udelson, J. E.; Gheorghiade, M. Dual vasopressin V1a/V2 antagonism: the next step in neurohormonal modulation in patients with heart failure? *J. Card. Failure* **2018**, *24*, 112−114.
(84) Tachibana, M.; Kagitani-Shimono, K.; Mohri, I.; Yamamoto, T.; Sanefuji, W.; Nakamura, A.; Oishi, M.; Kimura, T.; Onaka, T.; Ozono, K.; Taniike, M. Long-term administration of intranasal oxytocin is a safe and promising therapy for early adolescent boys with autism spectrum disorders. *J. Child Adolesc. Psychopharmacol.* **2013**, *23*, 123−127.
(85) Umbricht, D.; Del Valle Rubido, M.; Hollander, E.; McCracken, J. T.; Shic, F.; Scahill, L.; Noeldeke, J.; Boak, L.; Khwaja, O.; Squassante, L.; Grundschober, C.; Kletzl, H.; Fontoura, P. A single dose, randomized, controlled proof-of-mechanism study of a novel vasopressin 1a receptor antagonist (RG7713) in high-functioning adults with autism spectrum disorder. *Neuropsychopharmacology* **2017**, *42*, 1914−1923.
(86) Passoni, I.; Leonzino, M.; Gigliucci, V.; Chini, B.; Busnelli, M. Carbetocin is a functional selective Gq agonist that does not promote oxytocin receptor recycling after inducing β-arrestin-independent internalisation. *J. Neuroendocrinol.* **2016**, *28*(4), doi: DOI: 10.1111/jne.12363.
(87) Griffante, C.; Green, A.; Curcuruto, O.; Haslam, C. P.; Dickinson, B. A.; Arban, R. Selectivity of d[Cha4]AVP and SSR149415 at human vasopressin and oxytocin receptors: evidence that SSR149415 is a mixed vasopressin V1b/oxytocin receptor antagonist. *Br. J. Pharmacol.* **2005**, *146*, 744−751.
(88) Karpenko, I. A.; Klymchenko, A. S.; Gioria, S.; Kreder, R.; Shulov, I.; Villa, P.; Mély, Y.; Hibert, M.; Bonnet, D. Squaraine as a bright, stable and environment-sensitive far-red label for receptor-specific cellular imaging. *Chem. Commun. (Cambridge, U. K.)* **2015**, *51*, 2960−2963.
(89) Tahtaoui, C.; Guillier, F.; Klotz, P.; Galzi, J.-L.; Hibert, M.; Ilien, B. On the use of nonfluorescent dye labeled ligands in FRET-based receptor binding studies. *J. Med. Chem.* **2005**, *48*, 7847−7859.
(90) Zwier, J. M.; Roux, T.; Cottet, M.; Durroux, T.; Douzon, S.; Bdioui, S.; Gregor, N.; Bourrier, E.; Oueslati, N.; Nicolas, L.; Tinel, N.; Boisseau, C.; Yverneau, P.; Charrier-Savournin, F.; Fink, M.; Trinquet, E. A fluorescent ligand-binding alternative using Tag-lite® technology. *J. Biomol. Screening* **2010**, *15*, 1248−1259.
(91) Borthwick, A. D. Oral oxytocin antagonists. *J. Med. Chem.* **2010**, *53*, 6525−6538.
(92) Matthes, H. W.; Maldonado, R.; Simonin, F.; Valverde, O.; Slowe, S.; Kitchen, I.; Befort, K.; Dierich, A.; Le Meur, M.; Dollé, P.; Tzavara, E.; Hanoune, J.; Roques, B. P.; Kieffer, B. L. Loss of morphine-induced analgesia, reward effect and withdrawal symptoms in mice lacking the mu-opioid-receptor gene. *Nature* **1996**, *383*, 819−823.

DOI: 10.1021/acs.jmedchem.8b00697
J. Med. Chem. 2018, 61, 8670−8692